Gastroenterology 2018;154:1391–1404

Helicobacter pylori Depletes Cholesterol in Gastric Glands to Prevent Interferon Gamma Signaling and Escape the Inflammatory Response

Pau Morey,[1,*] **Lennart Pfannkuch**,[1,*] **Ervinna Pang**,[1,*] Francesco Boccellato,[1] Michael Sigal,[1,2] Aki Imai-Matsushima,[1] Victoria Dyer,[1] Manuel Koch,[1] Hans-Joachim Mollenkopf,[1] Philipp Schlaermann,[1] and **Thomas F. Meyer**[1,*]

[1]*Department of Molecular Biology, Max Planck Institute for Infection Biology, Berlin, Germany;* [2]*Department of Hepatology and Gastroenterology, Charité University Medicine, Berlin, Germany*

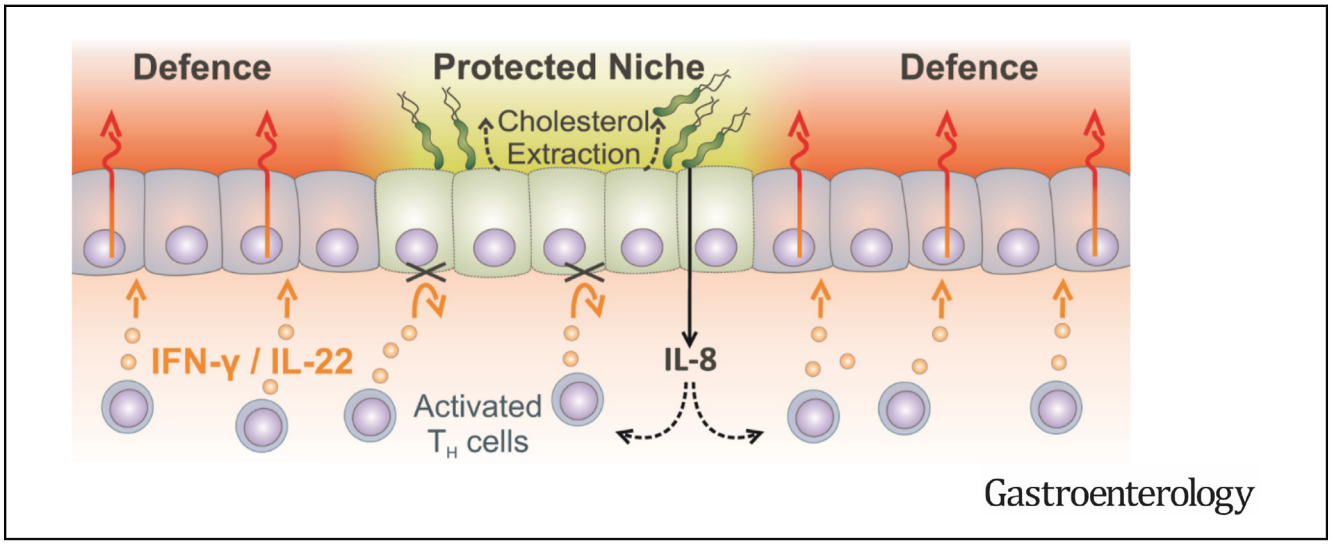

See Covering the Cover synopsis on page 1216.

BACKGROUND & AIMS: Despite inducing an inflammatory response, *Helicobacter pylori* can persist in the gastric mucosa for decades. *H pylori* expression of cholesterol-α-glucosyltransferase (encoded by *cgt*) is required for gastric colonization and T-cell activation. We investigated how cgt affects gastric epithelial cells and the host immune response. **METHODS:** MKN45 gastric epithelial cells, AGS cells, and human primary gastric epithelial cells (obtained from patients undergoing gastrectomy or sleeve resection or gastric antral organoids) were incubated with interferon gamma (IFNG) or interferon beta (IFNB) and exposed to *H pylori*, including *cag*PAI and *cgt* mutant strains. Some cells were incubated with methyl-β-cyclodextrin (to deplete cholesterol from membranes) or myriocin and zaragozic acid to prevent biosynthesis of sphingolipids and cholesterol and analyzed by immunoblot, immunofluorescence, and reverse transcription quantitative polymerase chain reaction analyses. We compared gene expression patterns among primary human gastric cells, uninfected or infected with *H pylori* P12 wt or P12Δ*cgt*, using microarray analysis. Mice with disruption of the IFNG receptor 1 (*Ifngr1*−/− mice) and C57BL6 (control) mice were infected with PMSS1 (wild-type) or PMSS1Δ*cgt H pylori*; gastric tissues were collected and analyzed by reverse transcription quantitative polymerase chain reaction or confocal microscopy. **RESULTS:** In primary gastric cells and cell lines, infection with *H pylori*, but not cgt mutants, blocked IFNG-induced signaling via JAK and STAT. Cells infected with *H pylori* were depleted of cholesterol, which reduced IFNG signaling by disrupting lipid rafts, leading to reduced phosphorylation (activation) of JAK and STAT1. *H pylori* infection of cells also blocked signaling by IFNB, interleukin 6 (IL6), and IL22 and reduced activation of genes regulated by these signaling pathways, including cytokines that regulate T-cell function (MIG and IP10) and anti-microbial peptides such as human β-defensin 3 (hBD3). We found that this mechanism allows *H pylori* to persist in proximity to infected cells while inducing inflammation only in the neighboring, non-infected epithelium. Stomach tissues from mice infected with PMSS1 had increased levels of IFNG, but did not express higher levels of interferon-response genes. Expression of the IFNG-response gene IRF1 was substantially higher in PMSS1Δ*cgt*-infected mice than PMSS1-infected mice. *Ifngr1*−/− mice were colonized by PMSS1 to a greater extent than control mice.

EDITOR'S NOTES

BACKGROUND AND CONTEXT

For reasons not well-understood, *Helicobacter pylori* can persist life-long in the stomach despite causing a strong inflammatory response, increasing the risk for serious sequelae such as ulcers and cancer.

NEW FINDINGS

By extracting cholesterol from host cells, *H pylori* blocks the assembly of IFN and other cytokine receptors, rendering the infected mucosa unable to respond properly to inflammatory signals from stroma and immune cells.

LIMITATIONS

Bacterial mutants for the *cgt* gene, which is required for cholesterol extraction, are unable to establish an in vivo infection, preventing a detailed analysis of its effects in the animal model.

IMPACT

This study provides important insight into the pitfalls of past vaccination approaches for *H pylori*. It also explains how cholesterol rich diet could negatively influence the inflammatory condition of the infected stomach mucosa.

CONCLUSIONS: *H pylori* expression of cgt reduces cholesterol levels in infected gastric epithelial cells and thereby blocks IFNG signaling, allowing the bacteria to escape the host inflammatory response. These findings provide insight into the mechanisms by which *H pylori* might promote gastric carcinogenesis (persisting despite constant inflammation) and ineffectiveness of T-cell–based vaccines against *H pylori*.

Keywords: JAK/STAT; IL-22; hBD3.

About half the world's population is chronically infected with the gram-negative bacterium *Helicobacter pylori*, which is implicated in severe gastric disease, including peptic ulcer and adenocarcinoma.[1] Colonization takes place in the gastric mucus and eventually involves bacterial adherence to the glandular epithelium.[2] The infection is characterized by a rapid and strong nuclear factor κB (NF-κB)–driven response,[3] which leads to the recruitment and activation of immune cells: CD4+ T cells, dominated by the Th1 lineage[4,5] play a decisive role in controlling the *Helicobacter* load via secretion of interferon gamma (IFNG).[6] This Th1 response is also fueled by type I IFNs (α/β) released from gastric epithelial cells themselves.[7] Th17 and Th22 T cells, characterized by interleukin (IL)17 and IL22 production, also promote the inflammatory milieu, helping to control infection.[8,9] Yet, *H pylori* is able to escape full elimination by host immunity through an unknown mechanism, resulting in a severe chronic inflammatory condition that represents a crucial aspect of its pathogenesis.

Gastric epithelial cells display receptors for type I (α/β) and type II (γ) interferons, the subunits of which (IFNAR1/IFNAR2 and IFNGR1/IFNGR2, respectively) are assembled in specialized cholesterol-rich membrane microdomains, known as lipid rafts.[10] Microdomain-dependent receptor activation[11] triggers JAK (Janus Kinase) and STAT (signaling transducer and activator of transcription) signaling via STAT1/2 phosphorylation and nuclear translocation to promote downstream expression of genes involved in inflammation and defense, including interferon regulatory factors (IRF), which further amplify the IFN response through positive feedback via STATs.[12] Gastric epithelial cells also express receptors for IL22[9], which can stimulate the production of antimicrobial factors that defend against mucosal pathogens.[13]

The effector mechanisms controlling colonization by *H pylori* remain sparsely understood. Epithelial cells can produce antimicrobial peptides (AMP), such as hBD3 (human β-defensin 3), which effectively kills *H pylori*[14,15] and is induced through MAPK (mitogen-activated protein kinase) and JAK/STAT signaling and stimulation with IFNG or IL22.[14,16–18] Strikingly, despite continued inflammation, hBD3 is not detected in infected human gastric biopsies.[15,19] We have previously shown that *H pylori* prevents hBD3 expression through a CagA (cytotoxin-associated gene A)-dependent mechanism.[14] However, how hBD3 remains blocked despite IFNG and IL22 stimulation is unclear.

H pylori, which is auxotroph for cholesterol, extracts the lipid from host membranes to incorporate it into its outer membrane as an α-glucosylated derivative, using the enzyme Cgt encoded by the gene HP0421 (*cgt*).[20–22] Cgt is the first in a series of *H pylori* enzymes that cause additional modifications to generate cholesteryl-6'-O-aycl-α-glucoside (αCAG) or cholesteryl-6'-O-phosphatidyl-α-glucoside (αCPG).[18] Cholesterol glucosylation and extraction from host cells result in lipid raft destruction and/or alteration of the membrane architecture,[21,22] which has been linked to immune evasion and bacterial persistence.[22–24] We previously reported that a cholesterol-rich diet leads to a reduction of the *H pylori* load concomitant with an increased Th1 response.[22]

Here, we provide insight into the underlying mechanism by showing that the IFN response is subverted by *H pylori* in gastric epithelial cells. This is caused by Cgt-dependent cholesterol depletion, resulting in the destruction of lipid rafts, failure of IFN receptor subunit assembly and, ultimately, lack of downstream signaling. Similarly, Cgt blocks IL6 and IL22 signaling. Our data provide evidence for the highly effective destruction of the responsiveness of *H pylori*-infected epithelium, even in the presence of strong

*** Authors share co-first authorship.**

Abbreviations used in this paper: **αCAG, cholesteryl-6'-O-aycl-α-glucoside; αCPG, cholesteryl-6'-O-phosphatidyl-α-glucoside; ALI, air-liquid interface; CagA, cytotoxin-associated gene A; hBD3, human β-defensin 3; IFN, interferon; IFNG, interferon gamma; IL, interleukin; IRF, interferon regulatory factors; JAK, Janus Kinase; mβCD, methyl-β-cyclodextrin; MAPK, mitogen-activated protein kinase; MOI, multiplicity of infection; NF-κB, nuclear factor κB; PEG, polyethylene glycol; RT-qPCR, reverse transcription quantitative polymerase chain reaction; STAT, signaling transducer and activator of transcription.**

Most current article

0016-5085
https://doi.org/10.1053/j.gastro.2017.12.008

cytokine signals from the adjacent micro-environment, thus impairing mucosal defense.

Materials and Methods

Ethical Permissions

Human gastric tissue specimens were obtained from individuals undergoing gastrectomy or sleeve resection, under the ethics approval by the Charité Ethics Committee (EA1/058/11 and EA1/129/12). Animal experiments were performed in mice maintained under pathogen-free conditions based on approval by the Ethics Committee for Animal Experimentation of the State of Berlin (G0205/12).

Cell Culture Infection and Treatment

Bacteria were collected from plates and resuspended in RPMI 1640 (serum-free). All cells were grown to 60% confluency, washed twice with phosphate-buffered saline, and serum starved with RPMI 1640 for 16 hours prior to experiments. Infection was carried out under serum-starved conditions at 37 °C, 5% CO_2 for the indicated times at multiplicity of infection (MOI) 20 or 50. Treatment with methyl-β-cyclodextrin (mβCD; Sigma, St. Louis, MO) was carried out for 5 hours at indicated concentrations. Biosynthesis of sphingolipids and cholesterol was inhibited by treating cells with myriocin (50 μmol/L; Sigma) for 72 hours and zaragozic acid (50 μmol/L, Cayman Chemical: Ann Arbor, MI) for the last 18 hours. In selected experiments, bacteria were treated with water-soluble cholesterol (Sigma) at 1 mg/mL for 1 hour prior to infection. Alternatively, polyethylene glycol (PEG)-cholesterol (10 mg/mL; Sigma) was added to cultures during the last hour of infection, while mock-infected cells were treated with an equal volume containing cholesterol. After infection, recombinant human IFNG (R&D Systems: Minneapolis, MN; 10 ng/mL), IFNB (PBL Assay Science, Piscataway, NJ; 2300 U/mL), IL6 (Peprotech, Rocky Hill, NJ; 25 ng/mL) or IL22 (Peprotech; 50 ng/mL) were added to selected wells and maintained for indicated times until the end of the experiment.

Primary Gastric Epithelial Air-Liquid Interface Cultures. Cells from organoids or freshly isolated glands were seeded in trans-well inserts (Millipore (Merck): Darmstadt, GE; PIHP01250) in 24-well plates and wells filled with 400 μL primary cell culture medium. Once cells had formed a confluent monolayer, medium on top of the cells was removed to start air-liquid interface (ALI) culture. Cultures were kept at 37°C, 5% CO_2 in a humidified incubator. Ten days later cells were infected by placing 50 μL of bacteria in phosphate-buffered saline (MOI 100) on top of the filters for 3 days.

For further information see Supplementary Materials and Methods. All RT-qPCR primers listed in Supplementary Table 1.

Data Deposition. Microarray data have been deposited in the Gene Expression Omnibus (GEO; www.ncbi.nlm.nih.gov/geo/) of the National Center for Biotechnology Information under GEO accession number GSE76589.

Results

H pylori *Blocks JAK/STAT Signaling upon IFNG Treatment*

To assess the influence of *H pylori* on the response to IFNG, we infected MKN45 gastric epithelial cells with strains P12 and P1 for 6 or 24 hours, followed by treatment with IFNG for 30 minutes. Immunoblotting revealed STAT1 phosphorylation in response to IFNG treatment in non-infected cells, cells infected with heat-killed bacteria, and cells infected for 6 hours (Figure 1*A*). Surprisingly, after prolonged infection (24 hours) IFNG stimulation failed to activate STAT1, irrespective of the *H pylori* strain (Figure 1*A*). To analyze the dynamics of this phenotype, we performed a time course experiment, showing that STAT1 phosphorylation was diminished after 16 hours and completely blocked from 24 until 96 hours of infection with P12 (Supplementary Figure 1*A*). To investigate the underlying mechanisms, we thus chose the 24 hour time point of infection as a reference. In AGS cells, too, 24 hours of infection inhibited the response to IFNG (Supplementary Figure 1*B*). MOI 10 was sufficient to partially block IFNG signaling in MKN45 cells within 24 hours and a complete block was observed with MOI 50 (Supplementary Figure 1*C*), which was therefore chosen for further experiments.

Upon IFNG stimulation, an activated IFNGR complex phosphorylates JAK1 and JAK2 kinases, which in turn phosphorylate STAT1. After 24 hours of infection with P12 or P1, neither JAK1 nor JAK2 was phosphorylated any more in MKN45 cells (Figure 1*B* and 1*C*, middle panel; Supplementary Figure 1*D*). Notably, JAK1 (Figure 1*B*) and JAK2 (data not shown) were activated in non-infected MKN45 cells even without IFNG stimulation; however, this was also diminished after infection. Infection conditions did not compromise cell viability (Supplementary Figure 1*E*).

Cgt is Required for Inactivation of IFNG-JAK/STAT1 Pathway

To identify the bacterial factor involved in the block of IFNG signaling, we infected MKN45 cells with *H pylori* wild type and mutant strains. As a recent report linked CagA translocation to STAT1 dephosphorylation via SHP-2 activation,[25] we tested deletion mutants for *cag*PAI, which encodes the entire type IV secretion system, *cagA* and *cgt*. While the *cagA* and *cag*PAI mutant strains still inhibited JAK/STAT1 signaling upon IFNG stimulation, the *cgt* mutant did not (Figure 1*D* and Supplementary Figure 1*B*). Immunofluorescence analysis showed that P12Δ*cgt* (Figure 1*C* and Supplementary Figure 1*D*) did not block JAK2 activation upon IFNG treatment, despite adhering to epithelial cells at levels comparable to wild type. Similarly, STAT1 signaling upon IFNG treatment was still inhibited in a Cgt-dependent manner at 48 h.p.i. (Supplementary Figure 1*F*). Although genetic complementation of the *cgt*-mutant strain only partially reconstituted Cgt expression (Supplementary Figure 1*G*), it was enough to restore the ability to impair JAK/STAT1 activation (Figure 1*E*) in MKN45 cells. Finally, we evaluated the consequences of disrupted JAK/STAT1 signaling by analyzing expression of downstream genes after IFN treatment, by infecting MKN45 cells for 24 hours with P12 wild type or P12Δ*cgt* prior to treatment with IFNG for 2.5 or 5 hours, followed by reverse transcription–quantitative polymerase chain reaction (RT-qPCR). Expression of IRF1, as well as the T-cell attractant chemokines MIG

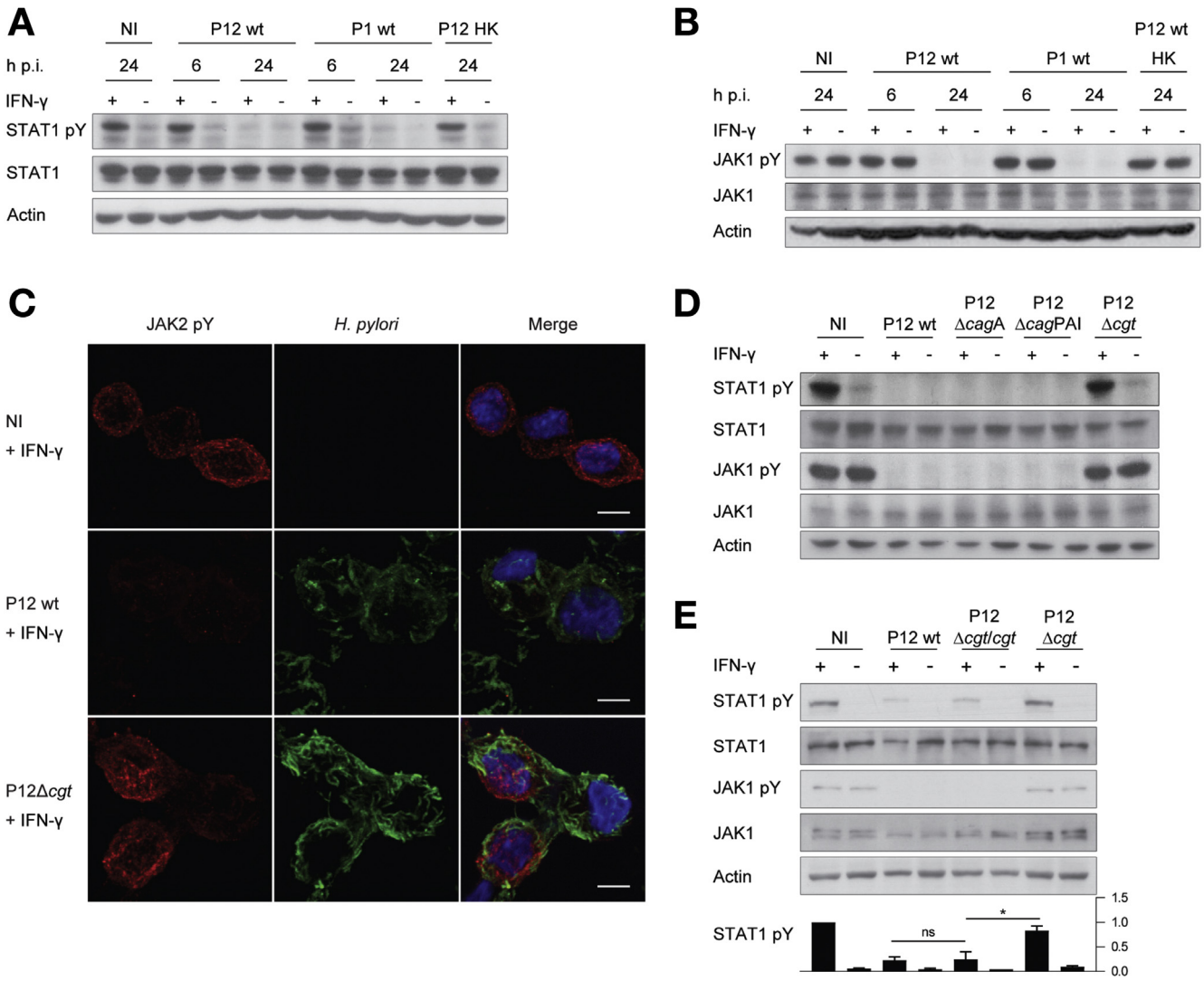

Figure 1. Prolonged infection prevents IFNG-induced activation of JAK1, JAK2, and STAT1 through Cgt activity. MKN45 cells were infected with the indicated strains (HK, heat killed) at MOI 50 and treated (+) or mock-treated (-) with IFNG (10 ng/mL, 30 minutes) at the indicated times post-infection (p.i.). (*A* and *B*) Immunoblot analysis of total protein level and phosphorylation of JAK1 or STAT1, respectively. (*C*) Analysis of JAK2 phosphorylation (red) by confocal IF, maximum projection. Cells were non-infected (NI) or infected with indicated *H pylori* strains (green) and treated with IFNG (10 ng/mL, 30 minutes). Scale bar = 5 μm. (*D* and *E*) Immunoblot analysis JAK1 and STAT1 phosphorylation and total protein levels of MKN45 cells infected or mock-infected (NI) for 24 hours at MOI 50 with the indicated *H pylori* strains and treatment with IFNG (10 ng/mL, 30 minutes).

and IFNG-inducible protein 10 (IP)-10 (encoded by CXCL9 and CXCL10 genes, respectively), was strongly up-regulated in non-infected cells upon IFNG treatment (Supplementary Figure 1*H*). Cells infected with P12Δ*cgt* also responded to IFNG, but after infection with wt P12 the response was significantly reduced. Accordingly, Cgt activity blocks the JAK/STAT1 pathway, as well as transcription of downstream genes involved in amplification of the IFNG response.

Inhibition of IFNG Response is Linked to Host Cholesterol Depletion, Lipid Raft Disruption, and IFNGR Assembly

Cholesterol acquisition by *H pylori* has been linked to the destruction of lipid rafts in epithelial cells.[22] Lipid rafts serve as platforms for cell signaling cascades, including IFN signaling.[26] As previously described,[22] we observed cholesterol depletion in cells infected with wild-type *H pylori* (Supplementary Figure 2*A*). To connect this to the block of the IFNG response, we treated cells with mβCD, which depletes cholesterol from eukaryotic membranes. Treatment did not affect cellular viability (Supplementary Figure 2*B*) but impaired both JAK1 and STAT1 phosphorylation (Figure 2*A*). We also inhibited the biosynthesis of sphingolipids and cholesterol by combined treatment with myriocin and zaragozic acid to disrupt lipid raft function.[11] Myriocin and zaragozic acid treatment indeed significantly blocked the induction of IRF1 expression in response to IFNG (Supplementary Figure 2*C*). In addition, when we coated *H pylori* with water-soluble cholesterol before infection to abolish cholesterol transfer from host cells, they did not block the cellular response to IFNG treatment

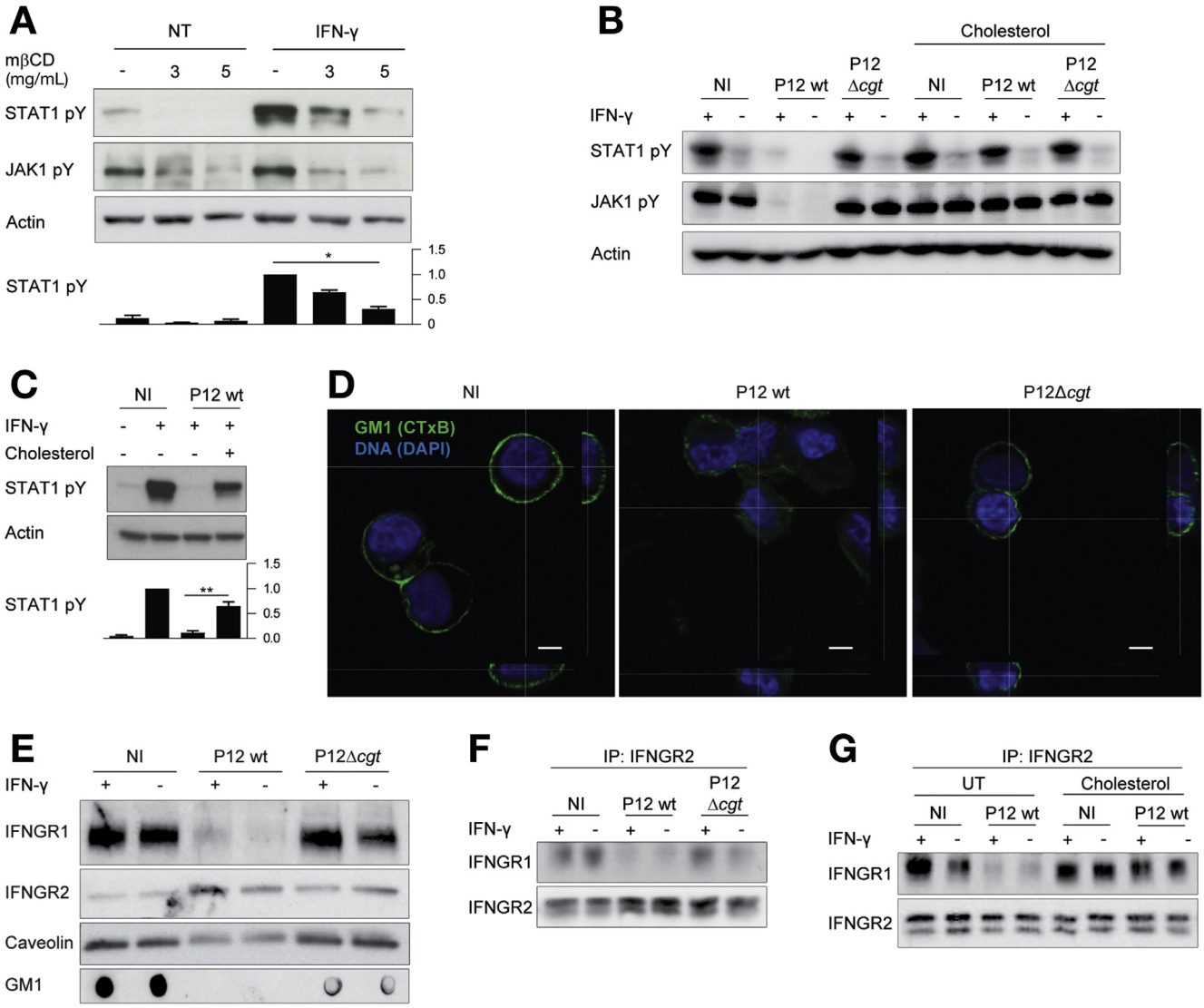

Figure 2. Cholesterol depletion by *H pylori* blocks IFNG signaling by disrupting lipid rafts, impairing IFNGR complex assembly. (*A*) Immunoblot analysis of JAK1/STAT1 phosphorylation after 5 hours mβCD treatment at indicated concentrations or in non-treated cells (-), with or without IFNG treatment (10 ng/mL, 30 minutes). (*B*) Immunoblot analysis of JAK1 and STAT1 phosphorylation upon IFNG treatment (+). MKN45 cells were infected for 24 hours with the indicated strains or non-infected, then treated with IFNG (+) (10 ng/mL, 30 minutes). Cholesterol-coating of bacteria was started 1 hour before infection and applied to non-infected cells accordingly. (*C*) Immunoblot analysis of STAT1 phosphorylation upon IFNG and/or PEG-cholesterol treatment. MKN45 cells were infected for 24 hours with *H pylori* wt or non-infected. In selected wells (+), PEG-cholesterol (5 mg/mL) was added during the final hour of infection. Then, cells were treated with IFNG (10 ng/mL, 30 minutes) (+) or mock-treated (-). Quantification: band intensity ratio STAT1pY:actin. (*D*) Confocal microscopy analysis (x-y sections with lateral views along dotted lines: x-z, bottom; y-z right) of the lipid raft marker GM1 (green) in membranes of cells non-infected or infected for 24 hours with indicated strains. Nuclei stained with DAPI (blue). Scale bar: 5 μm. (*E*) Immunoblot analysis of detergent-resistant membranes for IFNGR1, IFNGR2, caveolin, or dot blot analysis with CTxB-HRP. Cells were non-infected or infected for 24 hours with indicated strains, followed by treatment (+) or mock-treatment (-) with IFNG (10 ng/mL, 30 minutes). (*F* and *G*) Immunoprecipitation (IP) and immunoblot analysis of IFNGR subunits 1 and 2. IFNGR2 was pulled down using IFNGR2 antibody. MKN45 cells were infected with *H pylori* P12 wt or coated with water-soluble cholesterol before infection. Results representative of 2 independent experiments.

(Figure 2*B*). Cholesterol coating also restored the capacity of wt *H pylori*-infected cells to up-regulate IRF1 in response to IFNG, at levels comparable to non-infected cells (Supplementary Figure 2*D*). Cholesterol coating did not affect bacterial viability (Supplementary Figure 2*E*). To control for any effects on the initial host-pathogen interplay (eg, by masking bacterial adhesins), we repeated the experiment by adding PEG-cholesterol to the medium during the last hour of infection. This partially rescued the capacity of infected cells to respond to IFNG treatment, further highlighting the importance of cholesterol as a mediator of inflammation in response to *H pylori* (Figure 2*C*).

The IFNGR subunits 1 and 2 need to merge at cholesterol-rich micro-domains[11] to respond to IFNG

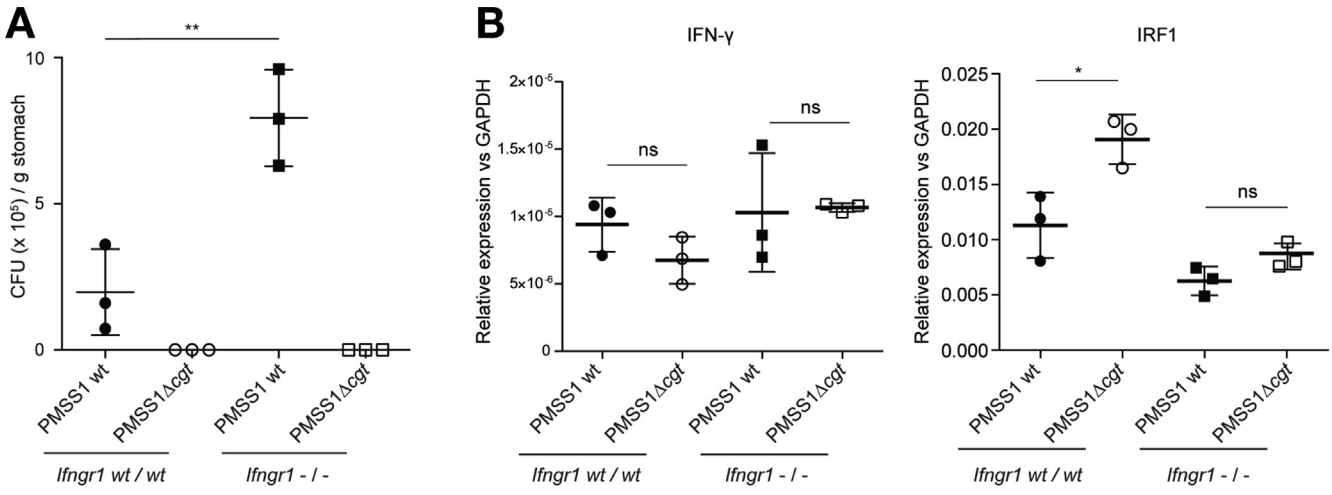
A
**
CFU (x 10⁵) / g stomach
10
5
0
PMSS1 wt
PMSS1ΔcgT
PMSS1 wt
PMSS1ΔcgT
Ifngr1 wt / wt
Ifngr1 - / -
B
IFN-γ
Relative expression vs GAPDH
2x10⁻⁵
1.5x10⁻⁵
1x10⁻⁵
5x10⁻⁶
0
ns
ns
IRF1
0.025
0.020
0.015
0.010
0.005
0.000
*
ns

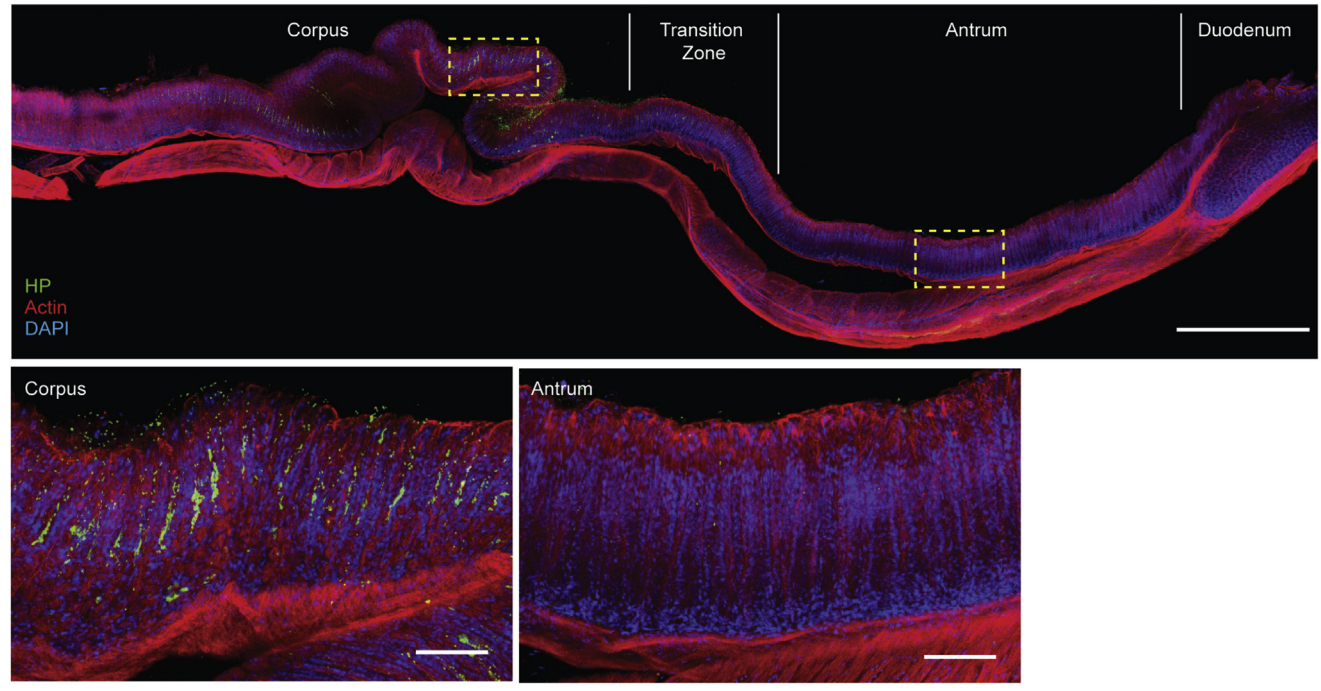
C
Corpus
Transition Zone
Antrum
Duodenum
HP
Actin
DAPI
Corpus
Antrum

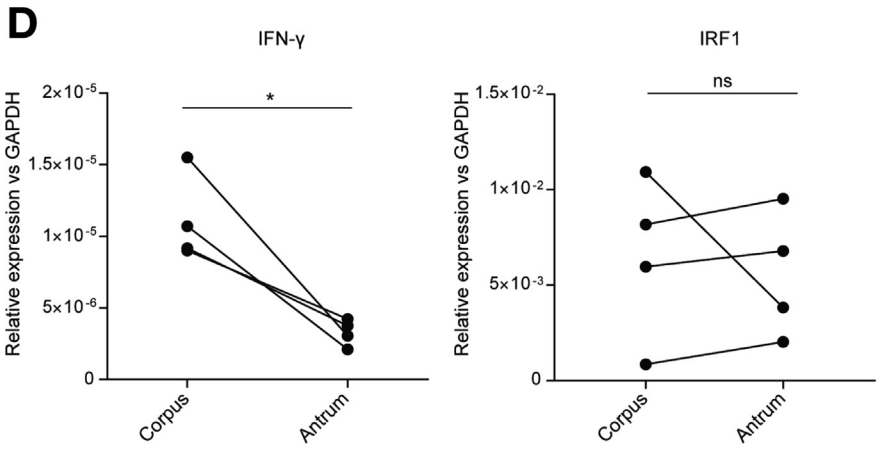
D
IFN-γ
IRF1
Relative expression vs GAPDH
2x10⁻⁵
1.5x10⁻⁵
1x10⁻⁵
5x10⁻⁶
0
*
1.5x10⁻²
1x10⁻²
5x10⁻³
ns
Corpus
Antrum

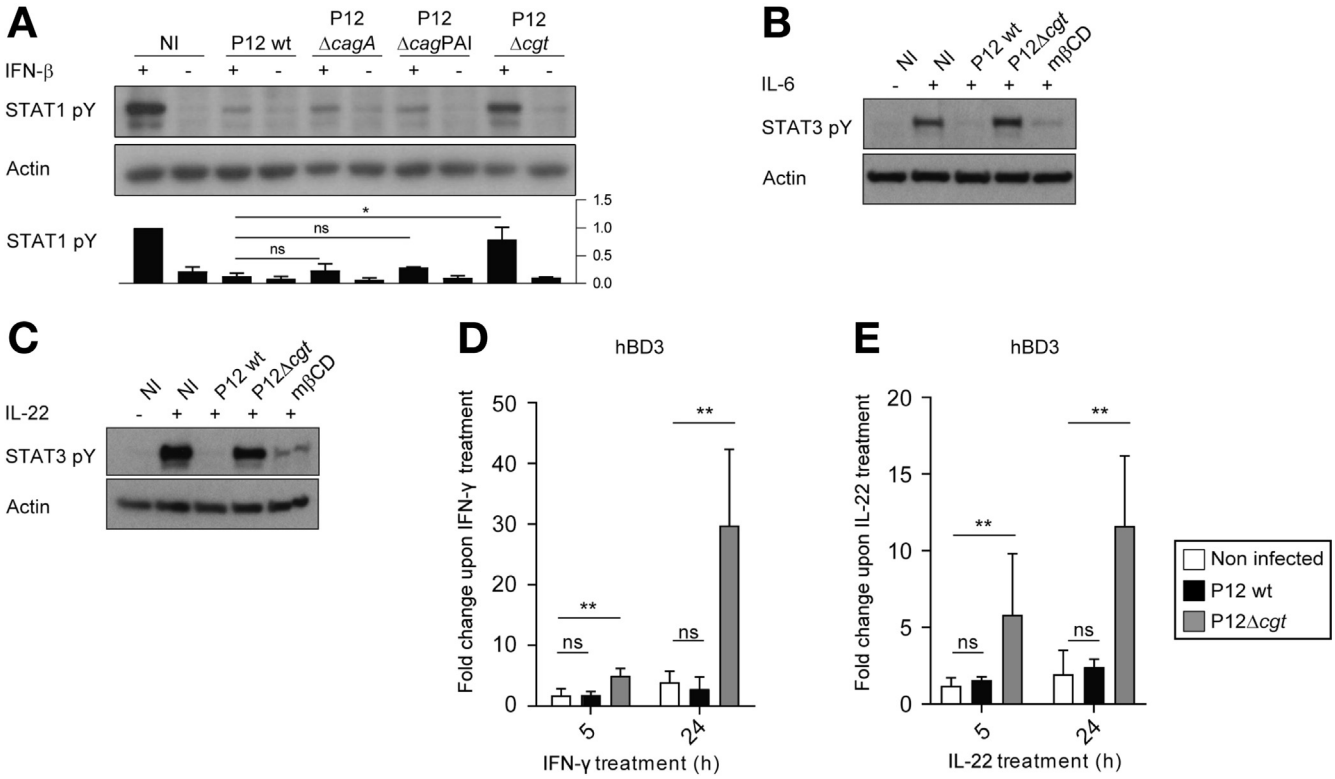

Figure 4. Cgt prevents IFNB-, IL6-, and IL22-induced signaling in epithelial cells upon prolonged infection and impairs hBD3 expression. (*A*) Immunoblot analysis of STAT1 pathway activation in MKN45 cells. Cells were infected for 24 hours with indicated strains or non-infected, then treated (+) or mock-treated (-) with IFNB (2300 U/mL) for 30 minutes. (*B* and *C*) Immunoblot analysis of STAT3 activation in MKN45 cells infected for 24 hours with indicated strains or treated with mβCD (5 mg/mL) for 5 hours, followed by 30 minutes with (*B*) IL6 (100 ng/mL) or (*C*) IL22 (50 ng/mL). (*D* and *E*) RT-qPCR analysis of hBD3. MKN45 cells were non-infected or infected with indicated strains for 24 hours. IFNG (10 ng/mL) (*D*) or IL22 (50 ng/mL) (*E*) were then added to selected wells for the specified times. To represent the net response to cytokines, results are normalized against relative gene expression of corresponding non-infected, P12 wt and P12Δ*cgt* infected cells. Data represented as mean ± SD. ns, non-significant, $^{**}P < .01$.

stimulation and initiate downstream signaling via JAK1 and JAK2.[10,27] We investigated the impact of *H pylori* on the integrity of lipid rafts by assessing potential alterations in the assembly of functional IFNGR. According to immunofluorescence analysis, surface accumulation of glycosphingolipid ganglioside GM1, a constituent marker of lipid rafts, is lost after infection with P12 wt and P12Δ*cagA* (Figure 2*D*, quantification of the relative membrane GM1 signal in Supplementary Figure 2*F*). In contrast, infection with P12Δ*cgt* did not notably alter GM1 distribution (Figure 2*D* and Supplementary Figure 2*F*). In addition, we performed a membrane fractionation to separate lipid rafts as detergent-resistant membranes. In control cells, fractions containing cholesterol-rich micro-domains, identified by the presence of raft markers GM1 or caveolin, partitioned in top fractions (Supplementary Figure 2*G*). Combining these fractions for Western blot analysis showed that GM1 as well as IFNGR1 were lost in detergent-resistant membranes upon infection with wild-type P12 but not P12Δ*cgt*, regardless of IFNG treatment (Figure 2*E*). In total lysates, IFNGR1 and IFNGR2 were detected in all conditions (Supplementary Figure 2*H*). Finally, we performed immunoprecipitation of IFNGR subunit 2 to test co-precipitation of IFNGR1. Immunoprecipitation specificity was controlled for by absence of the transferrin receptor CD71, a protein not associated with lipid rafts or the IFNGR complex (Supplementary Figure 2*I*). In line with recent findings,[11] MKN45 cells showed constitutive oligomerization of IFNGR subunits even in the absence of IFNG (Figure 2*F*). Despite this, prolonged wt *H pylori* infection but not

Figure 3. IFN response triggered by *H pylori* in vivo is ineffective. (*A*) Bacterial clearance in C57BL6 wt and Ifngr1 -/- mice orally infected with PMSS1 wt or PMSS1Δ*cgt*. Each point represents CFU counts for individual mice. Mean ± SD is also represented. $^{**}P < .01$. (*B*) RT-qPCR analysis of IFNG and IRF1 expression in stomachs of infected wt and Ifngr1 -/- mice, shown as fold-change to respective expression of mGAPDH. Data represented as mean ± SD. ns, non-significant, $^{*}P < .05$. (*C*) Confocal microscopy image of longitudinal stomach sections of mice orally infected with PMSS1 for 2 weeks, labelled for actin (phalloidin, red), *H pylori* (green), and nuclei (DAPI, blue). Scale bars: 1000 μm (upper) and 100 μm (lower). (*D*) RT-qPCR analysis of IFNG and IRF1 expression in samples taken from corpus or antrum of the mice used in (*C*), results represented as in (*B*).

P12Δ*cgt* abolished assembly of receptor subunits. Coating *H pylori* with exogenous cholesterol prior to infection restored assembly of IFNGR subunits (Figure 2*G*). Together, these data suggest that subversion of JAK/STAT1 signaling by *H pylori* takes place at the very top of the pathway, by preventing assembly of IFNG receptor subunits through lipid raft destruction.

H pylori *Blocks the IFNG Response In Vivo in a Cgt-Dependent Manner*

Reportedly, *H pylori cgt* mutants are unable to colonize mice.[21,22] Because Cgt activity is required for the block of the IFNG response, which in turn protects against *H pylori* in vivo,[6] we investigated whether the IFNG response is linked to bacterial clearance. After 3 days of infection PMSS1Δ*cgt* was already undetectable in wild-type mice (Figure 3*A*). Mice infected with PMSS1 or PMSS1Δ*cgt* presented similar IFNG levels in the stomach; however, the induction of the IFNG downstream response gene IRF1 was substantially higher in PMSS1Δ*cgt*-infected mice (Figure 3*B*). Next, we infected mice for 2 weeks with PMSS1 to allow a stronger Th1 response to develop. We observed a corpus-predominant gland occupation by *H pylori* in all analyzed mice (Figure 3*C*). Notably, the IFNG expression (Figure 3*D*, left) was higher compared with the less colonized antrum. However, IRF1 expression remained at similar levels (Figure 3*D*, right). Infection with wild-type *H pylori* thus leads to increased levels of IFNG, but fails to increase expression of interferon response genes, consistent with the notion of a Cgt-dependent block. Finally, although we reasoned that *H pylori* PMSS1Δ*cgt* might be able to infect *Ifngr1*-knock out mice (Figure 3*A*, right), this was not the case. Knockout mice did show increased colonization by wild-type PMSS1, indicating that additional defense-related pathways apart from IFNG might contribute to the clearance of PMSS1Δ*cgt*.

Cholesterol Depletion by H pylori *Inhibits Type I IFN, IL6, and IL22 Signaling and Downstream hBD3 Response*

Lipid raft integrity is also known to be required for type I IFNs and IL6 signaling.[10,28] In congruence, we observed that *H pylori* P12 also inhibited IFNB-induced STAT1 signaling in MKN45 cells, and this effect was dependent on the presence of *cgt* but not *cagA or cagPAI* (Figure 4*A*). Also, mβCD treatment inhibited IFNB signaling in a dose-dependent manner (Supplementary Figure 3*A*). Similarly, wild-type infection and mβCD treatment, but not infection with the *cgt* mutant, prevented STAT3 phosphorylation upon IL6 treatment (Figure 4*B*). IL22 is a crucial cytokine for mediating the epithelial defense against mucosal pathogens. Binding to receptors in epithelial cells triggers STAT3 activation, inducing expression of antimicrobial factors.[13] Again, 24-hour infection with wt P12 but not a P12Δ*cgt* mutant strain inhibited IL22 signaling transduction in epithelial cells (Figure 4*C*); the block was also observed upon mβCD treatment (Figure 4*C*). Genetic rescue of the *cgt* mutant partially restored the bacterial capacity to block IL22 signaling (Supplementary Figure 3*B*). Because IL22 signaling has not previously been reported to depend on cholesterol, we demonstrated restoration of IL22 signaling by adding PEG-cholesterol to MKN45 cells before IL22 stimulation (Supplementary Figure 3*C*).

Because IFNG and IL22 are reported to induce epithelial expression of hBD3,[29] a potent defensin against *H pylori*,[15,19] we tested the impact of infection on the cytokine-induced hBD3 response. Infection of MKN45 cells for 24 hours with P12Δ*cgt* but not P12 wt, followed by treatment with IFNG for 5 hours, induced a significant increase of hBD3 transcription (Figure 4*D*, left), which was even more dramatic after 24-hour IFNG treatment (Figure 4*D*, right). In contrast, the increase over time in non-infected and P12 wt-infected cells was minimal. Similarly, IL22 treatment also induced hBD3 expression in P12Δ*cgt*-infected cells, albeit to a lower extent, following a similar time course as IFNG (Figure 4*E*). In summary, *H pylori* blocks the production of hBD3 in epithelial cells stimulated with IFNG or IL22. Interestingly, co-stimulation with a *cgt*-deficient strain induced substantially higher hBD3 expression compared with cytokine treatment alone. Overall, these data confirm that cholesterol depletion by *H pylori* not only inhibits the response to IFNG, but also type I IFNs, IL6, and IL22.

Inhibition of JAK/STAT Signaling in Human Primary Gastric Epithelial Cells

We next used human gastric primary cultures[30,31] to validate our observations during authentic host-pathogen interaction. Cells derived from primary gastric antral organoids were seeded on plastic and infected with *H pylori* under serum starvation before IFNG or IFNB treatment for 30 minutes. Similar to results obtained with MKN45, *H pylori* P12, but not P12Δ*cgt*, prevented JAK1/STAT1 phosphorylation (Figure 5*A*). These differences were also observed at higher MOI and in cells isolated from the corpus region (Supplementary Figure 4*A*), independent of donors (Supplementary Figure 4*B*). In contrast to cancer cell lines, primary gastric epithelial cells did not exhibit constitutive JAK1 activation (Figure 5*A*). Block of IFNG signaling was observed at 24 hours post-infection, but not at earlier time points (Supplementary Figure 4*C*) or with a low MOI (Supplementary Figure 4*D*). Cholesterol-coated bacteria, however, failed to block JAK/STAT1 signaling (Figure 5*B*). Further, block of IFN signaling, as determined by the up-regulation of the type II IFN-activated gene CXCL9 in response to IFNG stimulation, was observed in *H pylori* P12 wt, P12Δ*cagA*, P12Δ*cag*PAI, or P12Δ*vacA*, but not in P12Δ*cgt*-infected cells (Supplementary Figure 4*E*). Moreover, *H pylori* P12 wt, but not P12Δ*cgt*, inhibited STAT3 phosphorylation upon IL22 treatment at 24 hours post-infection (Figure 5*C*). Genetic rescue of P12Δ*cgt* restored its capacity to block the response to IFNG and IL22 in primary epithelial cells (Supplementary Figure 4*F* and *G*).

To assess the global cellular response to infection with *H pylori* P12 wt or P12Δ*cgt,* we performed microarray analysis with human primary gastric cells infected with P12 wt or P12Δ*cgt*. Gene Ontology term enrichment analysis revealed responsiveness for genes involved in 'response to

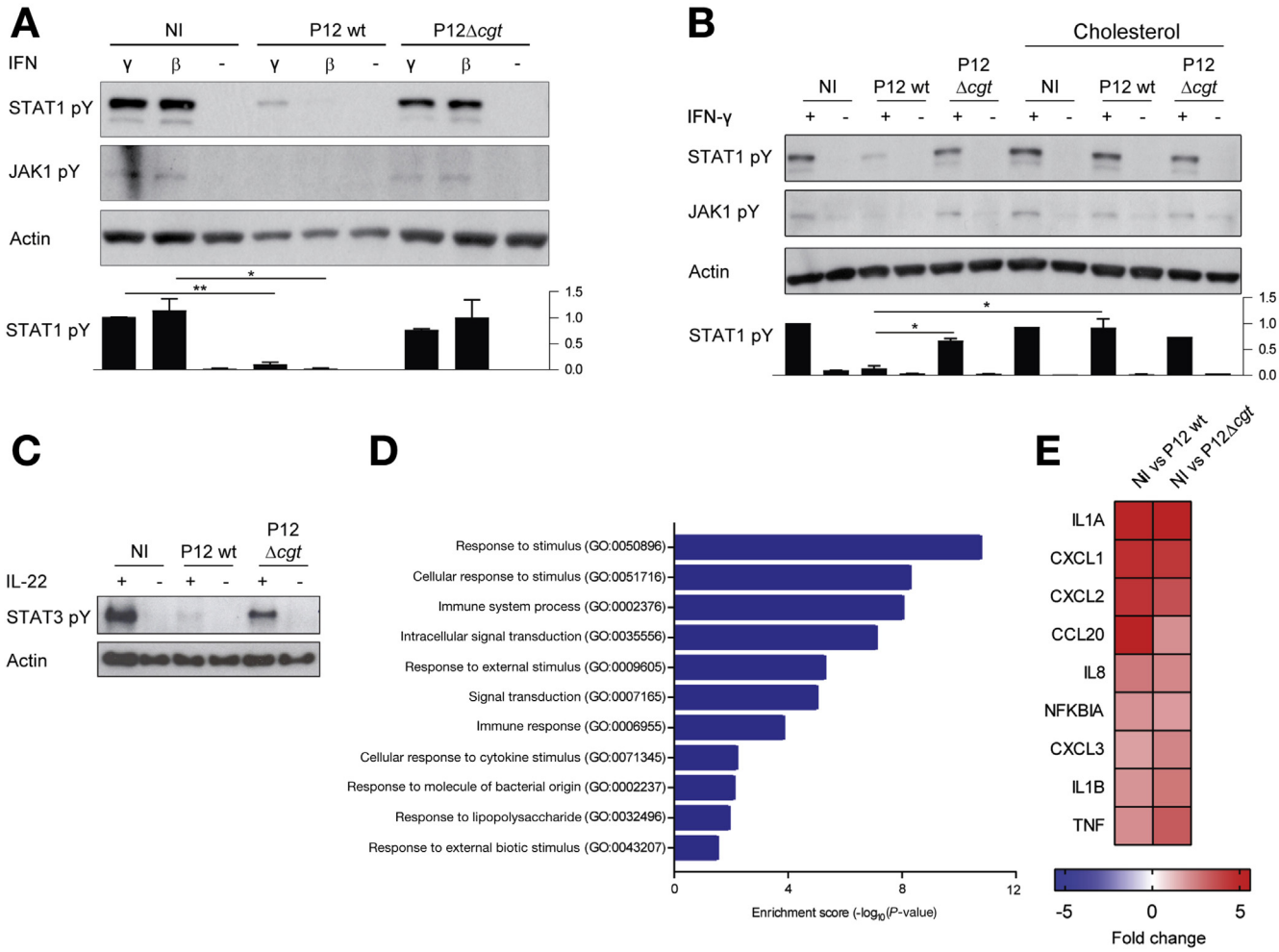

Figure 5. Cgt blocks IFN signaling in primary gastric epithelial cells. Human primary gastric cells were infected with indicated strains at MOI 20 for 24 hours or non-infected. (*A*) Immunoblot analysis of JAK1/STAT1 pathway activation. After infection cells from antrum were mock-treated or treated for 30 minutes with IFNG (5 ng/mL) or IFNB (2300 U/mL). Quantification: band intensity ratio STAT1pY: actin. (*B*) Cholesterol-coating of bacteria was started 1 hour before infection and applied to non-infected cells accordingly. Afterwards cells were mock-treated or treated for 30 minutes with IFNG (5 ng/mL). Result representative of 2 independent experiments. (*C*) Immunoblot analysis of STAT3 activation. Cells from antrum were infected for 24 hours with indicated strains and after infection treated for 30 minutes with IL22 (50 ng/mL). (*D* and *E*) Primary human cells were infected with *H pylori* P12 wt or P12Δ*cgt* for 26.5 hours and microarray results compared with those obtained in non-infected (n.i.) cells. Results shown are from 2 independent experiments with cells obtained from 2 independent donors. (*D*) Gene Ontology processes enrichment (Panther) from up-regulated genes in n.i. vs. P12 wt data set. In all cases $P < .05$. (*E*) NF-κB-response genes differentially modulated in n.i. vs. P12 wt and n.i. vs P12Δ*cgt* datasets. In all cases, fold change > 1.5 and P value $< .05$.

external stimuli,' 'signal transduction,' and 'immune response,' which was similar for both wt and P12Δ*cgt*-infected cells (Figure 5*D*, and data not shown). Many of the pro-inflammatory genes up-regulated upon infection with either strain are related to NF-κB signaling (Figure 5*E*). Therefore, while *H pylori* effectively blocks the response to IFNG, IFNB, and IL22 in normal human gastric epithelial cells, initial sensing of the pathogen by NF-κB[3] remains largely unaffected.

H pylori *Generates Micro-Niches of Diminished Inflammatory Response*

To spatially resolve the effects *H pylori* exerts, we examined the resulting cellular phenotypes over longer periods of time using a novel infection model of human gastric primary cells in air-liquid interphase culture.[32] This model enables longer infection times and resembles the in vivo situation more closely because it features greater cell type diversity, a protective layer of mucin, and cell polarization (Supplementary Figure 5*A*). After 3 days of infection with P12 wt at MOI 100, cells were treated with IFNG for 30 minutes and analyzed by immunofluorescence. Interestingly, IFNG treatment led to nuclear translocation of phospho-STAT1 (Figure 6*A*, middle panel). Micro-colonies of spiral-shaped bacteria (red) formed infection foci (Figure 6*B* and Supplementary Figures 5*A* and *B*) correlating with areas of reduced phospho-STAT1 exhibition (Figure 6*A*, bottom panel). At lower magnification, areas of reduced STAT1 activation appeared to clearly correlate with infected areas,

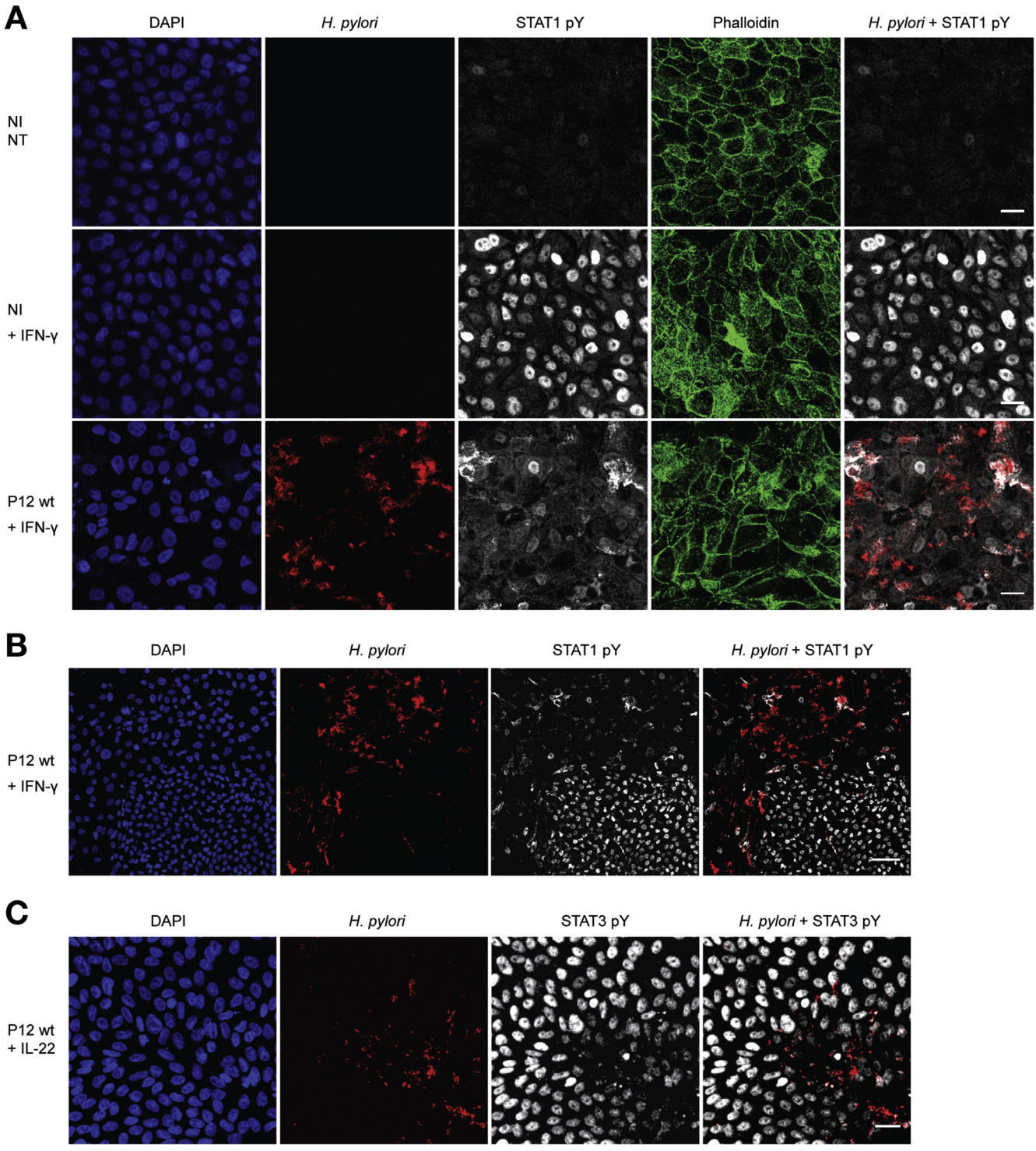

Figure 6. Block of cytokine responses in infected ALI cultures. Primary human cells grown on filters were infected with P12 wt at MOI 100 for 3 days or mock-infected (NI), then mock-treated or treated for 30 minutes with IFNG (10 ng/mL) (*A* and *B*) or IL22 (50 ng/mL) (*C*) and fixed with PFA. Filters were labelled with DAPI (DNA, blue) and antibodies against *H pylori* (red) and analyzed by whole-mount IF. (*A*) Analysis of STAT1 phosphorylation. Filters were labelled with phalloidin (green) and STAT1-pY (white). Scale bar: 20 μm. (*B*) Analysis of STAT1 phosphorylation, lower magnification. Filters were labelled with antibodies against STAT1-pY (white). Scale bar: 50 μm. (*C*) Analysis of STAT3 phosphorylation. Filters were labelled with antibodies against STAT3-pY (white). Scale bar: 20 μm.

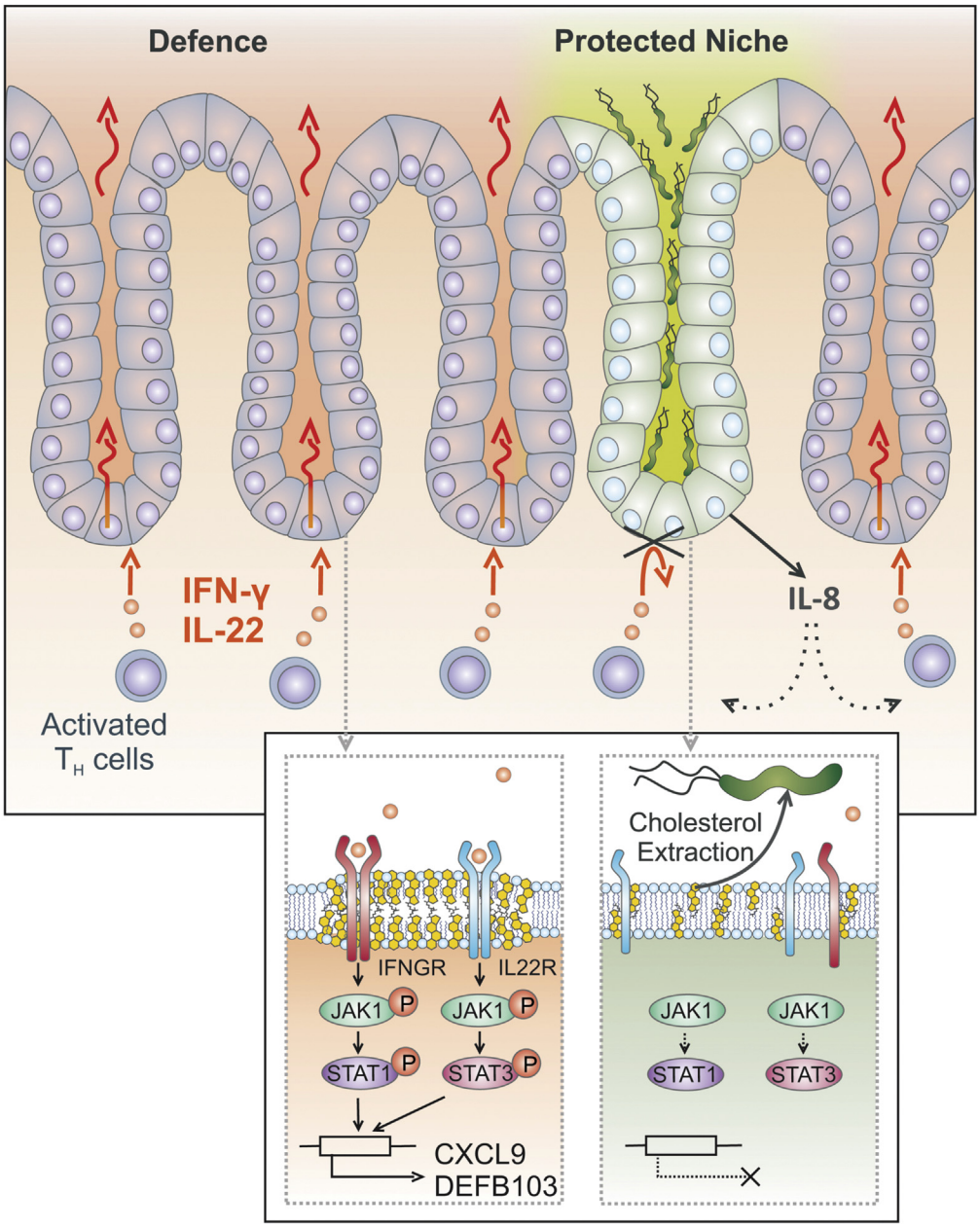

Figure 7. Summary of cholesterol-dependent subversion of immune response. Extraction of host cell cholesterol by H pylori's Cgt disrupts lipid rafts and thereby prevents assembly of IFNG receptors. In infected cells this leads to a shutdown of JAK/STAT1 signaling, inhibiting the production of T-cell chemo-attractants and antimicrobial peptides like hBD3. With this mechanism, *H pylori* creates micro-niches of locally diminished inflammation, despite a marked global immune response.

while non-infected areas of the same filter responded normally to IFNG (Figure 6*B*). Next, we quantified the number of phospho-STAT1–positive cells in infected compared with non- or less well-infected microscopic fields of the same filter. The vast majority of infected areas displayed phospho-STAT1 levels below the activation threshold, while non-infected fields exhibited a robust IFNG response (Supplementary Figure 5*C*). Infection with the P12Δ*cgt* mutant at MOI 200 led to similar colonization densities, yet the infected monolayer exhibited full STAT1 phosphorylation upon IFNG similar to non-infected cells (Supplementary Figure 5*D*). Similarly, *H pylori* infection also hampered STAT3 phosphorylation upon IL22 treatment in infected areas (Figure 6*C*). Thus, using an advanced epithelial cell culture model, we demonstrate that *H pylori* prevents infected cells from responding to IFNG or IL22. This favors the formation of micro-colonies at micro-niches devoid of STAT1 or STAT3 activation. Although non-infected sites of the same culture retain full responsiveness, this does not halt micro-colony formation at protected sites.

Discussion

A hallmark of gastric infections with *H pylori* is the strong NF-κB–driven response of the epithelium. This initiates a chronic inflammatory condition fueled by the recruitment of immune cells, which produce IFNs[4,6] and other cytokines, including IL22.[13] These cytokines trigger a second wave of epithelial responses, characterized by the release of defensins and other bactericidal factors, to

restrict pathogen growth.[29] As we report here, *H pylori* evolved a powerful means to prevent infected epithelial cells from responding to this cytokine burst – shutting down bactericidal activity right at the site of infection. This intriguing phenomenon, exerted by the bacterial enzyme Cgt, is in line with previous observations that point to an unexplained inhibition of IFNG-induced nuclear translocation of STAT1 during *H pylori* infection.[33] Our findings now provide the mechanistic clue to our earlier characterization of *cgt* as a critical determinant of *H pylori* immune evasion.[22]

The gastric mucosa of patients exhibits a marked prevalence of pro-inflammatory cytokines and mediators that provoke innate and Th1-, Th17-, and Th22-driven immune responses.[8,9,34,35] However, IFNG and IL17 merely control, rather than clear, established infections. Similarly, IL22 induces the production of relevant antimicrobial factors in gastric epithelial cells, but surprisingly IL22 knockout and wt mice show similar *H pylori* colonization rates.[18] Previous work identified the *H pylori* factors VacA and GGT as immune modulators that impair the activation and proliferation of T cells.[5,36] They skew normal T-cell maturation from Th1 and Th17 toward a Treg phenotype and thereby elicit a considerable degree of local and systemic tolerance.[37] Although this deficit of T-cell maturation can be rescued by vaccination, vaccine-driven T-cell activation normally achieves only a reduction of the bacterial load concomitant with an increased inflammation.[38] This paradox points to a block of the T-cell–mediated immunity at the effector side of host epithelial defense, which can be explained by the action of Cgt. Because Cgt acts only on infected cells, this gives rise to an intriguing scenario: while inflammation prevails in the infected tissue, Cgt generates protected islands of diminished defense, promoting pathogen survival. Indeed, this notion is corroborated by observations with chronically infected mice challenged with a secondary *H pylori* infection[39]: newly incoming bacteria were unable to colonize infected mice except for a few glands already occupied by the primary infection, pointing toward an overall anti-microbial environment in the infected stomach. Together these observations suggest that *H pylori* forms protected micro-niches surrounded by an otherwise inflamed and microbicidal milieu (Figure 7).

Amongst the T-cell chemotactic factors affected by Cgt are MIG and IP-10, which contribute to protection against *H pylori*.[7,40] Homeostasis of the mucosal colonization by *H pylori,* avoiding an excessive bacterial load, is thought to be achieved through secretion of a variety of innate factors, including defensins, mucins, and oxidative metabolites.[15,41,42] Many of these are produced by the epithelium in response to IFNG and IL22.[13,16,17] hBD3, one of the most potent factors against *H pylori,* is induced in an IFNG-dependent manner in the context of chronic gastrointestinal inflammation.[15,16] We have previously observed that EGFR-dependent induction of hBD3 is down-regulated upon translocation of *H pylori* CagA via the activation of SHP-2[14] and CagA-dependent activation of SHP-2 also interferes with IFNG signaling.[25] Thus, CagA acts synergistically with Cgt in preventing IFN signaling and hBD3 synthesis, with Cgt expressed also in strains that lack the *cag*PAI T4SS. Our results, however, show a minimal contribution of CagA in blocking JAK/STAT signaling, possibly because of variations in the active motifs of CagA proteins in our European strain as compared with Asian strains,[43] such as the one used by Wang and colleagues.[25] Consistently, biopsies from European patients exhibited poor bactericidal activity against *H pylori* and lack of hBD3, regardless of whether they were cagPAI/cagA positive or negative.[15,19]

Lipid rafts are also targeted by other pathogens known to block IFN signaling (such as West Nile virus), which modifies the distribution of lipid rafts in the membrane[44] and *Leishmania donovani,* which disrupts lipid rafts in macrophages to inhibit assembly of IFNGR subunits.[27] Here, using *H pylori*, we achieve striking mechanistic insights into microbial cholesterol depletion from host cells, an apparently common, yet little appreciated virulence strategy. Accordingly, cholesterol depletion prevents the partitioning of IFNGR1 to lipid rafts and association with IFNGR2 subunits.[27] In MKN45 cells, we observed an association of IFNGR2 and IFNGR1 subunits even in the absence of infection, consistent with the abnormal, constitutive JAK1/2 activation. However, this association collapsed upon *H pylori* infection, rendering these cells unresponsive, independently of the presence of interferons.

Our in vivo experiments confirmed a Cgt-dependent block of the IFNG response, with the results obtained in Ifngr1 knockout mice indicating that additional pathways contribute to preventing colonization with the PMSS1Δ*cgt* mutant. This finding is consistent with the inhibitory action of Cgt on multiple lipid raft-dependent pathways, including IL6 and IFNB,[10,28,44] and IL22, in addition to IFNG. Vice versa, Cgt may also cause receptor activation such as for EGFR and TGFBR, where cholesterol depletion increases the number of molecules available for ligand binding.[26,45,46] Apart from this, many signaling routes, particularly those involving the pro-inflammatory pathway NF-κB, appear to function normally in *H pylori*-infected cells, even at a time when cholesterol depletion has progressed.

We have substantiated our findings in primary epithelial cells from different donors. Importantly, the use of cells from human gastric organoids allowed us to address biological questions in a mutation-free background.[30] Although primary cell models are increasingly used to address questions of infection biology,[47] little data related to *H pylori* are available yet. Here, we also utilized an advanced ALI model, which offers several improvements: (i) cultures grow under the influence of Wnt to maintain stemness; (ii) cells differentiate toward a diversity of cells, including pit, neck, chief, parietal, and neuroendocrine cells; (iii) cell polarization and secretion of a protective mucus layer supports an authentic equilibrium between cells and bacteria, enabling long-term infection.[32]

As we have previously shown, dietary cholesterol supplementation significantly reduces the *H pylori* burden in mice.[22] The decreased colonization came at the cost of substantially increased IFNG-driven inflammation. Our current results, together with the established link between lipid rafts and IFN signaling,[10,27] are in complete agreement with

previous in vivo findings.[22] Accordingly, cholesterol supply in the context of *H pylori* infection enhances JAK/STAT signaling together with the release of antibacterial effectors. Such increased Th1 responses, however, are also thought to promote preneoplastic lesions.[6,48] This notion, in turn, is consistent with the situation in patients suffering from increased blood cholesterol levels, especially in the form of low-density lipoprotein-cholesterol, who often exhibit severe *H pylori*-induced gastritis.[49] Accordingly, a low-cholesterol diet may reduce the pathology of *H pylori* gastric infections. This places Cgt function, cholesterol metabolism, and inflammation at the crossroads of gastric pathogenesis and cancer.

Supplementary Material

Note: To access the supplementary material accompanying this article, visit the online version of *Gastroenterology* at www.gastrojournal.org, and at https://doi.org/10.1053/j.gastro.2017.12.008.

References

1. Bauer B, Meyer TF. The human gastric pathogen helicobacter pylori and its association with gastric cancer and ulcer disease. Ulcers 2011;2011:1–23.
2. Sigal M, Rothenberg ME, Logan CY, et al. Helicobacter pylori activates and expands Lgr5(+) stem cells through direct colonization of the gastric glands. Gastroenterology 2015;148:1392–1404.e21.
3. **Zimmermann S, Pfannkuch L, Al-Zeer MA, Bartfeld S**, et al. ALPK1- and TIFA-dependent innate immune response triggered by the helicobacter pylori type IV secretion system. Cell Rep 2017;20:2384–2395.
4. Bamford KB, Fan X, Crowe SE, et al. Lymphocytes in the human gastric mucosa during Helicobacter pylori have a T helper cell 1 phenotype. Gastroenterology 1998;114:482–492.
5. Salama NR, Hartung ML, Muller A. Life in the human stomach: persistence strategies of the bacterial pathogen Helicobacter pylori. Nat Rev Microbiol 2013;11:385–399.
6. **Sayi A, Kohler E, Hitzler I**, et al. The CD4+ T cell-mediated IFN-gamma response to Helicobacter infection is essential for clearance and determines gastric cancer risk. J Immunol 2009;182:7085–7101.
7. Watanabe T, Asano N, Fichtner-Feigl S, et al. NOD1 contributes to mouse host defense against Helicobacter pylori via induction of type I IFN and activation of the ISGF3 signaling pathway. J Clin Invest 2010;120:1645–1662.
8. Horvath DJ Jr, Washington MK, Cope VA, et al. IL-23 Contributes to control of chronic Helicobacter pylori infection and the development of T helper responses in a mouse model. Front Immunol 2012;3:56.
9. **Zhuang Y**, Cheng P, **Liu XF**, et al. A pro-inflammatory role for Th22 cells in Helicobacter pylori-associated gastritis. Gut 2015;64:1368–1378.
10. Takaoka A, Mitani Y, Suemori H, et al. Cross talk between interferon-gamma and -alpha/beta signaling components in caveolar membrane domains. Science 2000;288:2357–2360.
11. **Blouin CM, Hamon Y, Gonnord P**, et al. Glycosylation-dependent IFN-gammaR partitioning in lipid and actin nanodomains is critical for JAK activation. Cell 2016;166:920–934.
12. Ivashkiv LB, Donlin LT. Regulation of type I interferon responses. Nat Rev Immunol 2014;14:36–49.
13. Zheng Y, Valdez PA, Danilenko DM, et al. Interleukin-22 mediates early host defense against attaching and effacing bacterial pathogens. Nat Med 2008;14:282–289.
14. Bauer B, Pang E, Holland C, et al. The Helicobacter pylori virulence effector CagA abrogates human beta-defensin 3 expression via inactivation of EGFR signaling. Cell Host Microbe 2012;11:576–586.
15. **Nuding S, Gersemann M**, Hosaka Y, et al. Gastric antimicrobial peptides fail to eradicate Helicobacter pylori infection due to selective induction and resistance. PLoS One 2013;8:e73867.
16. Fahlgren A, Hammarstrom S, Danielsson A, et al. beta-Defensin-3 and -4 in intestinal epithelial cells display increased mRNA expression in ulcerative colitis. Clin Exp Immunol 2004;137:379–385.
17. Joly S, Organ CC, Johnson GK, et al. Correlation between beta-defensin expression and induction profiles in gingival keratinocytes. Mol Immunol 2005;42:1073–1084.
18. Dixon BR, Radin JN, Piazuelo MB, et al. IL-17a and IL-22 induce expression of antimicrobials in gastrointestinal epithelial cells and may contribute to epithelial cell defense against Helicobacter pylori. PLoS One 2016;11:e0148514.
19. **Bauer B, Wex T**, Kuester D, et al. Differential expression of human beta defensin 2 and 3 in gastric mucosa of Helicobacter pylori-infected individuals. Helicobacter 2013;18:6–12.
20. **Lebrun AH, Wunder C, Hildebrand J**, et al. Cloning of a cholesterol-alpha-glucosyltransferase from Helicobacter pylori. J Biol Chem 2006;281:27765–27772.
21. Wang HJ, Cheng WC, Cheng HH, et al. Helicobacter pylori cholesteryl glucosides interfere with host membrane phase and affect type IV secretion system function during infection in AGS cells. Mol Microbiol 2012;83:67–84.
22. **Wunder C, Churin Y, Winau F**, et al. Cholesterol glucosylation promotes immune evasion by Helicobacter pylori. Nat Med 2006;12:1030–1038.
23. Beigier-Bompadre M, Moos V, Belogolova E, et al. Modulation of the CD4+ T-cell response by Helicobacter pylori depends on known virulence factors and bacterial cholesterol and cholesterol alpha-glucoside content. J Infect Dis 2011;204:1339–1348.
24. **Du SY, Wang HJ**, Cheng HH, et al. Cholesterol glucosylation by Helicobacter pylori delays internalization and arrests phagosome maturation in macrophages. J Microbiol Immunol Infect 2016;49:636–645.
25. Wang YC, Chen CL, Sheu BS, et al. Helicobacter pylori infection activates Src homology-2 domain-containing phosphatase 2 to suppress IFN-gamma signaling. J Immunol 2014;193:4149–4158.
26. **Arish M, Husein A**, Kashif M, et al. Orchestration of membrane receptor signaling by membrane lipids. Biochimie 2015;113:111–124.
27. Sen S, Roy K, Mukherjee S, et al. Restoration of IFN-gammaR subunit assembly, IFNgamma signaling and

parasite clearance in Leishmania donovani infected macrophages: role of membrane cholesterol. PLoS Pathog 2011;7:e1002229.
28. Sehgal PB, Guo GG, Shah M, et al. Cytokine signaling: STATS in plasma membrane rafts. J Biol Chem 2002; 277:12067–12074.
29. Ostaff MJ, Stange EF, Wehkamp J. Antimicrobial peptides and gut microbiota in homeostasis and pathology. EMBO Mol Med 2013;5:1465–1483.
30. Schlaermann P, Toelle B, Berger H, et al. A novel human gastric primary cell culture system for modelling Helicobacter pylori infection in vitro. Gut 2016;65:202–213.
31. Bartfeld S, Bayram T, van de Wetering M, et al. In vitro expansion of human gastric epithelial stem cells and their responses to bacterial infection. Gastroenterology 2015; 148:126–136.e6.
32. Boccellato F, Woelffling S, Imai-Matsushima A, et al. Polarised epithelial monolayers of the gastric mucosa reveal insights into mucosal homeostasis and defence against infection. Gut 2018. https://doi.org/10.1136/gutjnl-2017-314540. [Epub ahead of print].
33. Mitchell P, Germain C, Fiori PL, et al. Chronic exposure to Helicobacter pylori impairs dendritic cell function and inhibits Th1 development. Infect Immun 2007;75:810–819.
34. Rad R, Dossumbekova A, Neu B, et al. Cytokine gene polymorphisms influence mucosal cytokine expression, gastric inflammation, and host specific colonisation during Helicobacter pylori infection. Gut 2004;53:1082–1089.
35. Wen S, Felley CP, Bouzourene H, et al. Inflammatory gene profiles in gastric mucosa during Helicobacter pylori infection in humans. J Immunol 2004;172: 2595–2606.
36. Gebert B, Fischer W, Weiss E, et al. Helicobacter pylori vacuolating cytotoxin inhibits T lymphocyte activation. Science 2003;301:1099–1102.
37. Oertli M, Noben M, Engler DB, et al. Helicobacter pylori gamma-glutamyl transpeptidase and vacuolating cytotoxin promote gastric persistence and immune tolerance. Proc Natl Acad Sci U S A 2013;110:3047–3052.
38. Koch M, Meyer TF, Moss SF. Inflammation, immunity, vaccines for Helicobacter pylori infection. Helicobacter 2013;18(Suppl 1):18–23.
39. Keilberg D, Zavros Y, Shepherd B, et al. Spatial and temporal shifts in bacterial biogeography and gland occupation during the development of a chronic infection. MBio 2016;7.
40. Flach CF, Mozer M, Sundquist M, et al. Mucosal vaccination increases local chemokine production attracting immune cells to the stomach mucosa of Helicobacter pylori infected mice. Vaccine 2012;30:1636–1643.
41. Ermak TH, Giannasca PJ, Nichols R, et al. Immunization of mice with urease vaccine affords protection against Helicobacter pylori infection in the absence of antibodies and is mediated by MHC class II-restricted responses. J Exp Med 1998;188:2277–2288.
42. Kawakubo M, Ito Y, Okimura Y, et al. Natural antibiotic function of a human gastric mucin against Helicobacter pylori infection. Science 2004;305:1003–1006.
43. Naito M, Yamazaki T, Tsutsumi R, et al. Influence of EPIYA-repeat polymorphism on the phosphorylation-dependent biological activity of Helicobacter pylori CagA. Gastroenterology 2006;130:1181–1190.
44. Mackenzie JM, **Khromykh AA, Parton RG**. Cholesterol manipulation by West Nile virus perturbs the cellular immune response. Cell Host Microbe 2007; 2:229–239.
45. Westover EJ, Covey DF, Brockman HL, et al. Cholesterol depletion results in site-specific increases in epidermal growth factor receptor phosphorylation due to membrane level effects. Studies with cholesterol enantiomers. J Biol Chem 2003;278:51125–51133.
46. Chen CL, Liu IH, Fliesler SJ, et al. Cholesterol suppresses cellular TGF-beta responsiveness: implications in atherogenesis. J Cell Sci 2007;120:3509–3521.
47. Bartfeld S. Modeling infectious diseases and host-microbe interactions in gastrointestinal organoids. Dev Biol 2016;420:262–270.
48. Syu LJ, El-Zaatari M, Eaton KA, et al. Transgenic expression of interferon-gamma in mouse stomach leads to inflammation, metaplasia, and dysplasia. Am J Pathol 2012;181:2114–2125.
49. Kucukazman M, Yavuz B, Sacikara M, et al. The relationship between updated Sydney System score and LDL cholesterol levels in patients infected with Helicobacter pylori. Dig Dis Sci 2009;54:604–607.

Author names in bold designate shared co-first authorship.

Received May 26, 2017. Accepted December 14, 2017.

Reprint requests
Address requests for reprints to: Prof Dr Thomas F. Meyer, Department of Molecular Biology, Max Planck Institute for Infection Biology, Charitéplatz 1, 10117 Berlin, Germany. e-mail: meyer@mpiib-berlin.mpg.de; fax: +49 30 28 460 401.

Acknowledgments
The authors thank Jörg Angermann, Kirstin Hoffmann, Stefanie Mülllerke, and Ina Wagner for technical assistance, Robert Hurwitz for generating the Cgt antibody, Toni Aebischer, Bianca Bauer, Michael Fehlings, June Ghosh-Guha, and Eric Perret for fruitful discussions, and Rike Zietlow for expert editing of the manuscript.

Author contributions
P.M., E.P., and L.P. designed and performed the experiments and analyzed the data; V.D. and M.K. performed the in vivo experiments; H.-J.M. analyzed the microarray data; P.S., F.B., M.S., A.I.M., M.K, and T.F.M. provided experimental guidance during the study; P.M., L.P., and T.F.M. wrote the manuscript; T.F.M. conceived the study and provided conceptual guidance.

Conflicts of interest
The authors disclose no conflicts.

Grant support
P.M. was supported by the People Programme (Marie Curie Actions) of the European Union's Seventh Framework Programme FP7/2007-2013/ under REA grant agreement no. 316682; E.P. and L.P. received support from the Deutsche Forschungsgemeinschaft through grant SFB633 to T.F.M.; M.S. was funded as a clinician scientist by the Berlin Institute of Health (BIH). The funders played no role in the design of the study or the collection, analysis, and interpretation of the data.

Transcript profiling
Microarray data have been deposited in the Gene Expression Omnibus (GEO; www.ncbi.nlm.nih.gov/geo/) of the National Center for Biotechnology Information and can be accessed with the GEO accession number GSE76589.

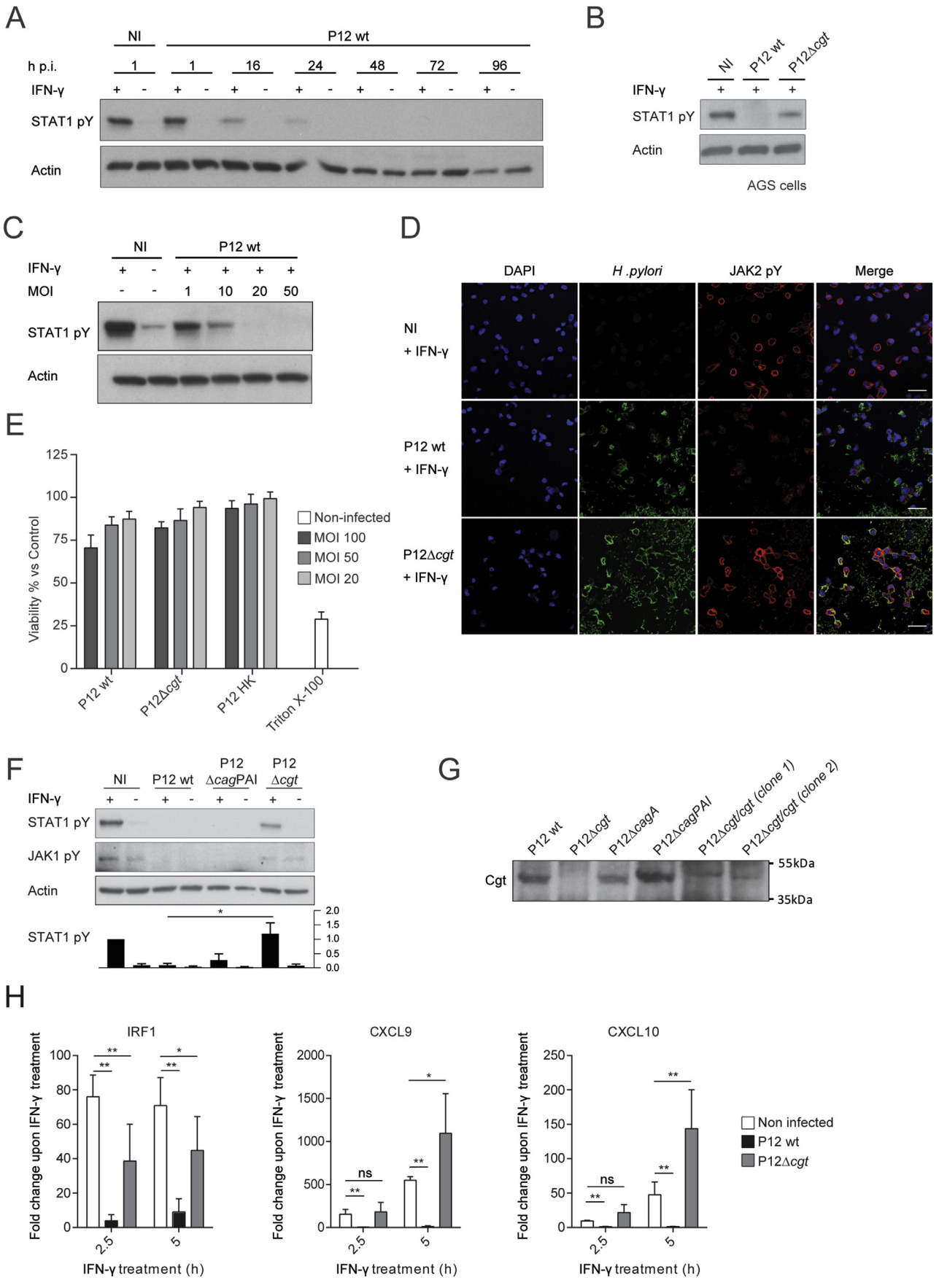
A
NI
P12 wt
h p.i.
1
1
16
24
48
72
96
IFN-γ
STAT1 pY
Actin
B
NI
P12 wt
P12Δcgt
IFN-γ
STAT1 pY
Actin
AGS cells
C
NI
P12 wt
IFN-γ
MOI
1
10
20
50
STAT1 pY
Actin
D
DAPI
H .pylori
JAK2 pY
Merge
NI
+ IFN-γ
P12 wt
+ IFN-γ
P12Δcgt
+ IFN-γ
E
Viability % vs Control
Non-infected
MOI 100
MOI 50
MOI 20
P12 wt
P12Δcgt
P12 HK
Triton X-100
F
NI
P12 wt
P12 ΔcagPAI
P12 Δcgt
IFN-γ
STAT1 pY
JAK1 pY
Actin
STAT1 pY
G
P12 wt
P12Δcgt
P12ΔcagA
P12ΔcagPAI
P12Δcgt/cgt (clone 1)
P12Δcgt/cgt (clone 2)
Cgt
55kDa
35kDa
H
IRF1
CXCL9
CXCL10
Fold change upon IFN-γ treatment
IFN-γ treatment (h)
Non infected
P12 wt
P12Δcgt

Supplementary Figure 1. (*A*) Time course analysis of IFNG induced STAT1 phosphorylation by immunoblot. MKN45 cells were infected with *H pylori* P12 wild type at MOI 50 or non-infected (NI). After indicated infection times, cells were treated (+) with IFNG (10 ng/mL, 30 minutes). (*B*) Immunoblot analysis of IFNG induced STAT1 phosphorylation in AGS gastric epithelial cell line upon infection with indicated *H pylori* strain at MOI 50 and in non-infected cells. After 24 hours of infection, cells were treated (+) with IFNG (10 ng/mL, 30 minutes). (*C*) MOI titration analysis of IFNG induced STAT1 phosphorylation by immunoblot. MKN45 cells were infected with *H pylori* P12 wild type at indicated MOIs or non-infected (NI). After 24 hours of infection, cells were treated (+) with IFNG (10 ng/mL, 30 minutes). (*D*) Analysis of JAK2 phosphorylation (red) by confocal IF at low magnification, confocal section. Cells were non-infected (NI), or infected with indicated *H pylori* strains (bacteria labeled in green). In all cases, cells were treated with IFNG (10 ng/mL, 30 minutes). Scale bar: 10 μm. The result is representative of 3 independent experiments. (*E*) Cellular viability of MKN45 cells infected with indicated *H pylori* strains, or heat-killed P12 (P12 HK) at indicated MOIs for 24 hours. Viability was measured via a fluorescence-based ATP assay (Promega, Madison, WI). All readings were normalized against non-infected (NI) cells. Cells treated for 5 minutes with Triton X-100 serve as control. Data shows mean ± SD of 2 independent biological experiments. SD is derived from 3 technical replicates. (*F*) Immunoblot analysis of IFNG induced JAK1 and STAT1 phosphorylation in MKN45 gastric epithelial cells after 48 hours of infection with indicated *H pylori* strains at MOI 50 and in non-infected cells. At the end of infection, cells were treated (+) or mock-treated (-) with IFNG (10 ng/mL) for 30 minutes. Quantification shows band intensity ratio of STAT1pY:actin. (*G*) Immunoblot analysis of CGT expression after genetic complementation of CGT mutant strain. $4x10^6$ bacteria of *H pylori* P12 wt, P12Δcgt, ΔcagA, ΔcagPAI, and 2 clones of the recomplemented strains Δcgt/cgt were lysed in Laemmli buffer and checked for CGT expression by using an in-house created monoclonal anti-CGT antibody. (*H*) Response to IFNG for genes IRF1, CXCL9, and CXCL10 quantified by RT-qPCR analysis. MKN45 cells were non-infected or infected with indicated *H pylori* strains for 24 hours. IFNG (10 ng/mL) was then added to selected wells for the specified times. To represent the net response to IFN, results were normalized against relative gene expression of corresponding non-infected, P12 and P12Δcgt infected cells. Data are represented as mean ± SD; ns, non-significant, $^*P < .05$, $^{**}P < .01$.

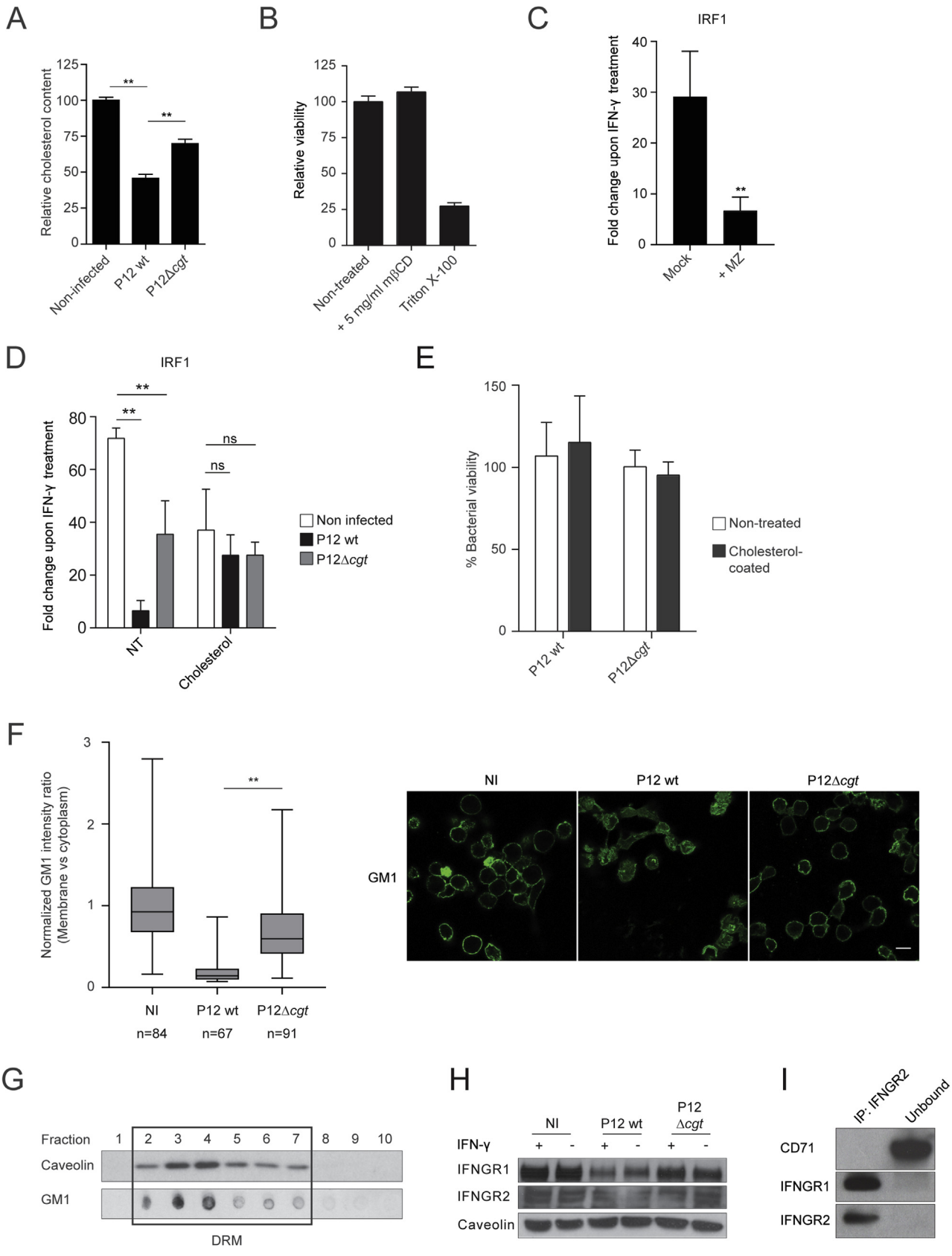
A
Relative cholesterol content
125
100
75
50
25
0
**
**
Non-infected
P12 wt
P12Δcgt
B
Relative viability
125
100
75
50
25
0
Non-treated
+ 5 mg/ml mβCD
Triton X-100
C
IRF1
Fold change upon IFN-γ treatment
40
30
20
10
0
**
Mock
+ MZ
D
IRF1
Fold change upon IFN-γ treatment
80
60
40
20
0
**
**
ns
ns
NT
Cholesterol
Non infected
P12 wt
P12Δcgt
E
% Bacterial viability
150
100
50
0
P12 wt
P12Δcgt
Non-treated
Cholesterol-coated
F
Normalized GM1 intensity ratio (Membrane vs cytoplasm)
3
2
1
0
**
NI
P12 wt
P12Δcgt
n=84
n=67
n=91
NI
P12 wt
P12Δcgt
GM1
G
Fraction 1 2 3 4 5 6 7 8 9 10
Caveolin
GM1
DRM
H
NI
P12 wt
P12 Δcgt
IFN-γ + - + - + -
IFNGR1
IFNGR2
Caveolin
I
IP: IFNGR2
Unbound
CD71
IFNGR1
IFNGR2

Supplementary Figure 2. (*A*) Cholesterol quantification of MKN45 upon *H pylori* infection. Cells were non-infected (NI) or infected with indicated strains of *H pylori* for 24 hours at MOI 50. After this period, cholesterol was quantified using Amplex kit (Invitrogen Carlsbad, CA). All readings were normalized against protein content and further normalized against cholesterol levels in non-infected cells. Data show mean ± SD of 2 independent biological experiments with 2 technical replicates each. (*B*) Cellular viability of MKN45 cells treated with mβCD (5 mg/mL) for 6 hours. Viability was measured via a fluorescence-based ATP assay (Promega). All readings were normalized against the NI and mock-treated cells. Cells treated for 5 minutes with TritonX-100 served as control. Data show mean ± SD of 2 independent biological experiments with 2 technical replicates each. (*C*) Response to 2.5-hour treatment with IFNG (10 ng/mL) after mock treatment or treatment with myriocin (72 hours, 50 μmol/L) plus zaragozic acid (18 hours, 50 μmol/L) (MZ). IRF1 mRNA levels obtained by qRT-PCR were normalized against respective GAPDH mRNA expression, and further normalized against non-infected (NI) cells. Data show mean ± SD of 2 independent biological experiments with 2 technical replicates each. For statistical analysis, MZ-treated samples were compared with mock, IFNG-treated controls: ns non-significant, $^{**}P < .01$. (*D*) Response to 2.5-hour treatment with IFNG for IRF1 gene in cells infected with bacteria with or without cholesterol coating. MKN45 cells were non-infected or infected with indicated *H pylori* strains for 24 hours. IFNG (10 ng/mL) was then added to selected wells for the 2.5 hours. To represent the net response to IFN, results were normalized against relative gene expression of respective corresponding non-infected, P12 and P12Δcgt infected cells. Data are represented as mean ± SD; ns, non-significant, $^{**}P < .01$. (*E*) Viability of cholesterol-coated bacteria. Bacteria (10^8/mL) in serum-free medium were coated or mock-coated with exogenous cholesterol (1 mg/mL) for 1 hour. Colony forming units (CFU)/mL were quantified 3 days later. Data are expressed as percentage bacterial survival relative to the untreated P12 (without cholesterol coating). Data show mean ± SD of 2 independent biological experiments with 2 technical replicates each. (*F*) Confocal microscopic analysis of the lipid raft marker GM1 (stained with CTxB-Alexa488, green) in cellular membranes of cells non-infected (NI) or infected for 24 hours with indicated *H pylori* strains. Left panel corresponds to the quantification of relative superficial GM1 signal. Results are shown as a box-plot (2nd and 3rd quartiles, median represented as horizontal line inside the box) of the ratio between cellular membrane and correspondent cytoplasm average intensities and further normalized to the average intensity ratio of non-infected cells of each corresponding experiment. Data correspond to 3 independent experiments; n = number of analyzed cells; $^{**}P < .01$. Right panel, representative images used for quantification. *Scale bar*: 10 μm. (*G*) Immunoblot analysis of detergent resistant membrane fractions (1–10, from top to bottom) of uninfected MKN45 cells after density gradient centrifugation for distribution of caveolin or GM1 distribution detected by dot blot with cholera toxin B conjugated to HRP. Fractions inside the box were pooled for further analysis. (*H*) Immunoblot analysis of whole cell lysate of MKN45 cells for IFNGR1, IFNGR2, or caveolin. Cells were non-infected (NI) or infected for 24 hours with indicated *H pylori* strains. After infection time, cells were treated (+) or mock-treated (-) with IFNG (10 ng/mL, 30 minutes). (*I*) Immunoprecipitation (IP) and immunoblot analysis of IFNGR subunits 1, 2, and CD71. IFNGR2 was pulled down using anti-IFNGR2 antibody.

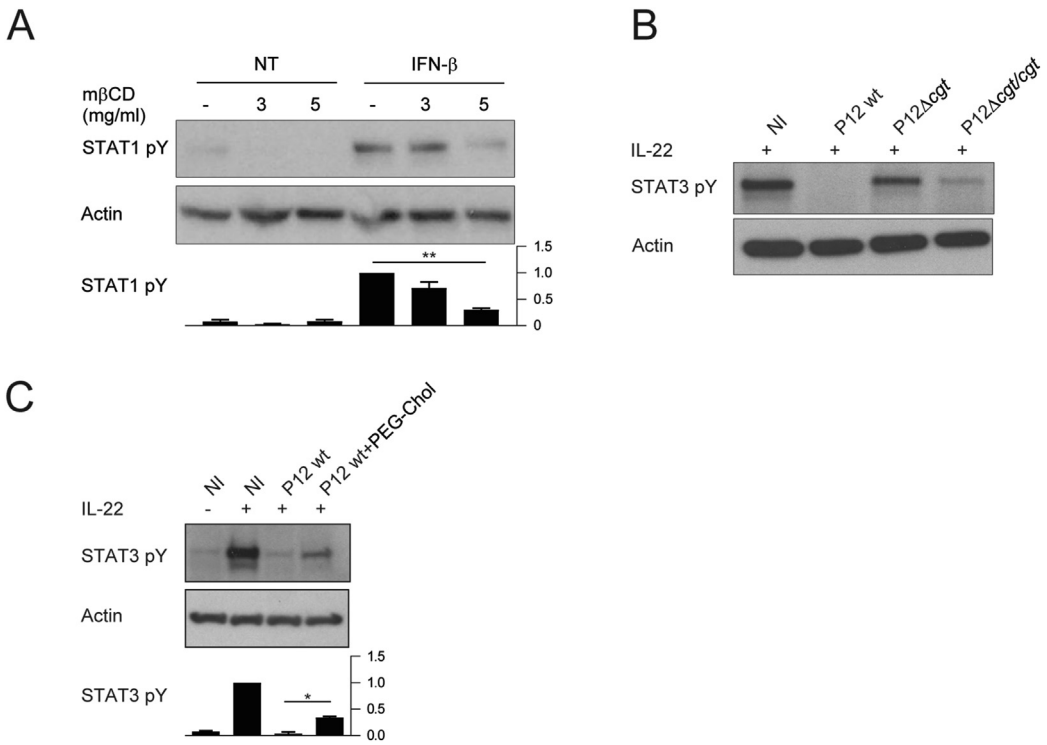

Supplementary Figure 3. (*A*) Immunoblot analysis of STAT1 phosphorylation after 5 hours mβCD treatment at the concentrations indicated or in non-treated cells (-). IFNB treatment (2300 U/mL, 30 minutes) was applied in selected wells. The result is representative of 3 independent experiments. Quantification shows band intensity ratio of STAT1pY:actin (*B*) Immunoblot analysis of STAT3 phosphorylation of MKN45 cells infected with indicated *H pylori* strains or mock-infected (NI) for 24 hours at MOI 50 with the indicated *H pylori* strains, followed by treatment with IL22 (50 ng/mL) for 30 minutes. (*C*) Immunoblot analysis of STAT3 activation in MKN45 cells. Cells were infected for 24 hours with *H pylori* P12 wild type or mock infected. In selected wells PEG-cholesterol was added during the final hour of infection. Cells were then treated with IL22 (50 ng/mL, 30 minutes) (+) or mock-treated (-). Quantification shows band intensity ratio of STAT1pY:actin.

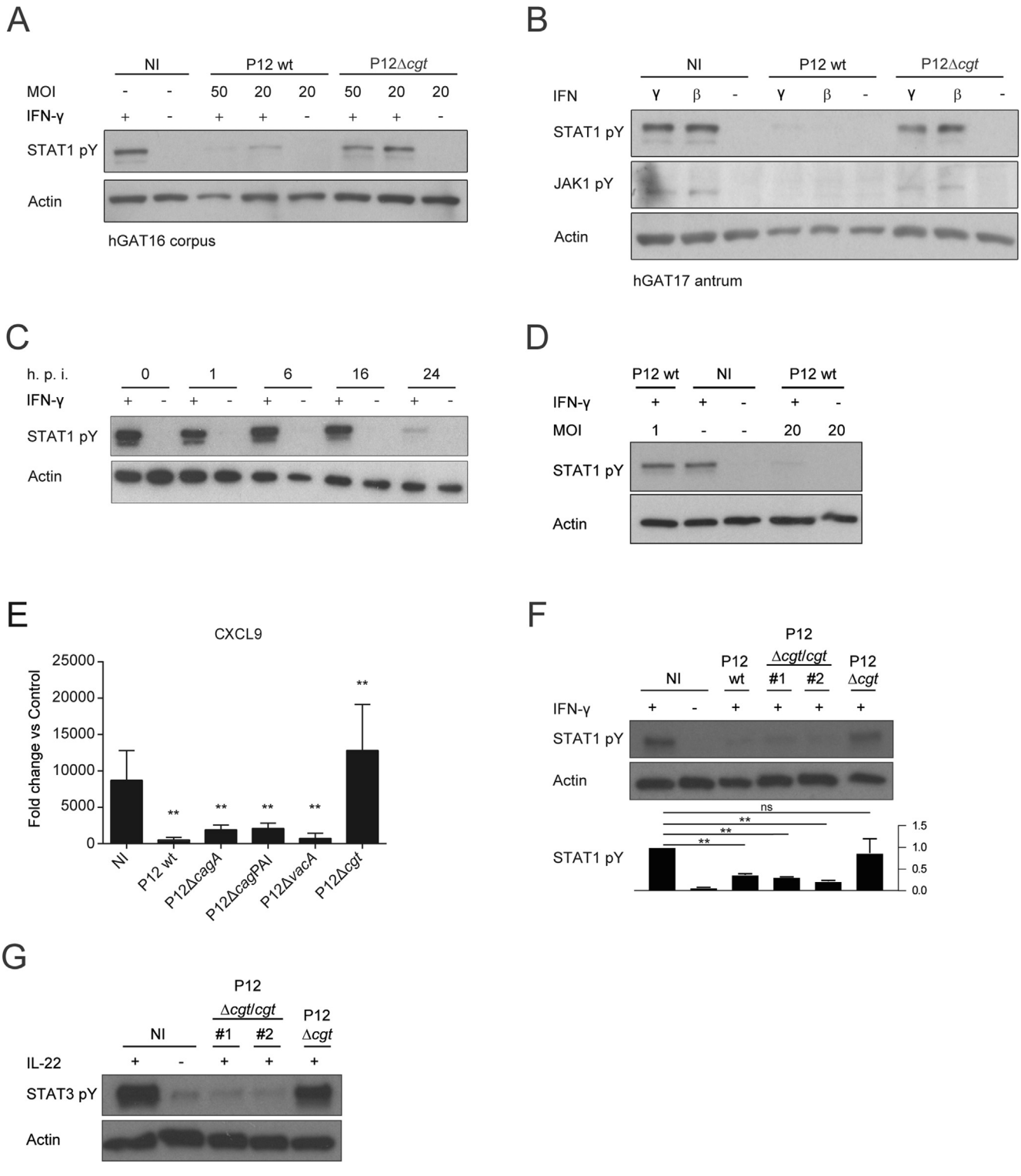
A
NI
P12 wt
P12Δcgt
MOI
IFN-γ
STAT1 pY
Actin
hGAT16 corpus
B
NI
P12 wt
P12Δcgt
IFN
STAT1 pY
JAK1 pY
Actin
hGAT17 antrum
C
h. p. i.
IFN-γ
STAT1 pY
Actin
D
P12 wt
NI
P12 wt
IFN-γ
MOI
STAT1 pY
Actin
E
CXCL9
Fold change vs Control
NI
P12 wt
P12ΔcagA
P12ΔcagPAI
P12ΔvacA
P12Δcgt
F
P12
NI
P12 wt
Δcgt/cgt
#1
#2
P12 Δcgt
IFN-γ
STAT1 pY
Actin
ns
STAT1 pY
G
P12
Δcgt/cgt
NI
#1
#2
P12 Δcgt
IL-22
STAT3 pY
Actin

Supplementary Figure 4. Experiment performed in 2D primary gastric human cells from different donors infected with indicated *H pylori* strains at MOI 20 or 50 for 24 hours or non-infected (NI). (*A*) Immunoblot analysis of STAT1 pathway activation. Cells from the corpus region were infected with indicated *H pylori* strains at different MOIs. After infection time cells were mock-treated or treated with IFNG (5 ng/mL). (*B*) Immunoblot analysis of the activation of JAK1/STAT1 pathway. After infection, cells were mock-treated or treated 30 minutes with IFNG (γ) (5 ng/mL) or IFNB (β) (2300 U/mL). (*C*) Time course analysis of IFNG-induced STAT1 phosphorylation by immunoblot. Cells were infected with *H pylori* P12 wt at MOI 20 or non-infected (NI). After indicated infection times, cells were treated ($+$) with IFNG (5 ng/mL, 30 minutes). (*D*) Immunoblot analysis of STAT1 phosphorylation. Cells were infected with *H pylori* wild type at different MOIs or left uninfected. After infection time cells were mock-treated or treated with IFNG (5 ng/mL). (*E*) Response to 2.5-hour treatment with IFNG (5 ng/mL) after infection with indicated *H pylori* strains or non-infected (NI). CXCL9 mRNA levels obtained by qRT-PCR were normalized against respective GAPDH mRNA levels, and further normalized against non-infected (NI) cells. Data show mean $\pm$ SD of 4 independent biological experiments (performed with cells from 2 different donors) with 2 technical replicates each. For statistical analysis, infected samples were compared with uninfected, IFNG-treated controls: ns non-significant, $^{**}P < .01$. Immunoblot analysis of STAT1 (*F*) or STAT3 (*G*) phosphorylation of primary cells mock-infected (NI) or infected with *H pylori* P12 wt, P12Δcgt or 2 clones of the recomplemented strains Δ*cgt*/*cgt* for 24 hours at MOI 50, followed by treatment with (*F*) IFNG (5 ng/mL, 30 minutes) or (*G*) IL22 (50 ng/mL, 30 minutes). Quantification of (*F*) shows band intensity ratio of STAT1pY:actin.

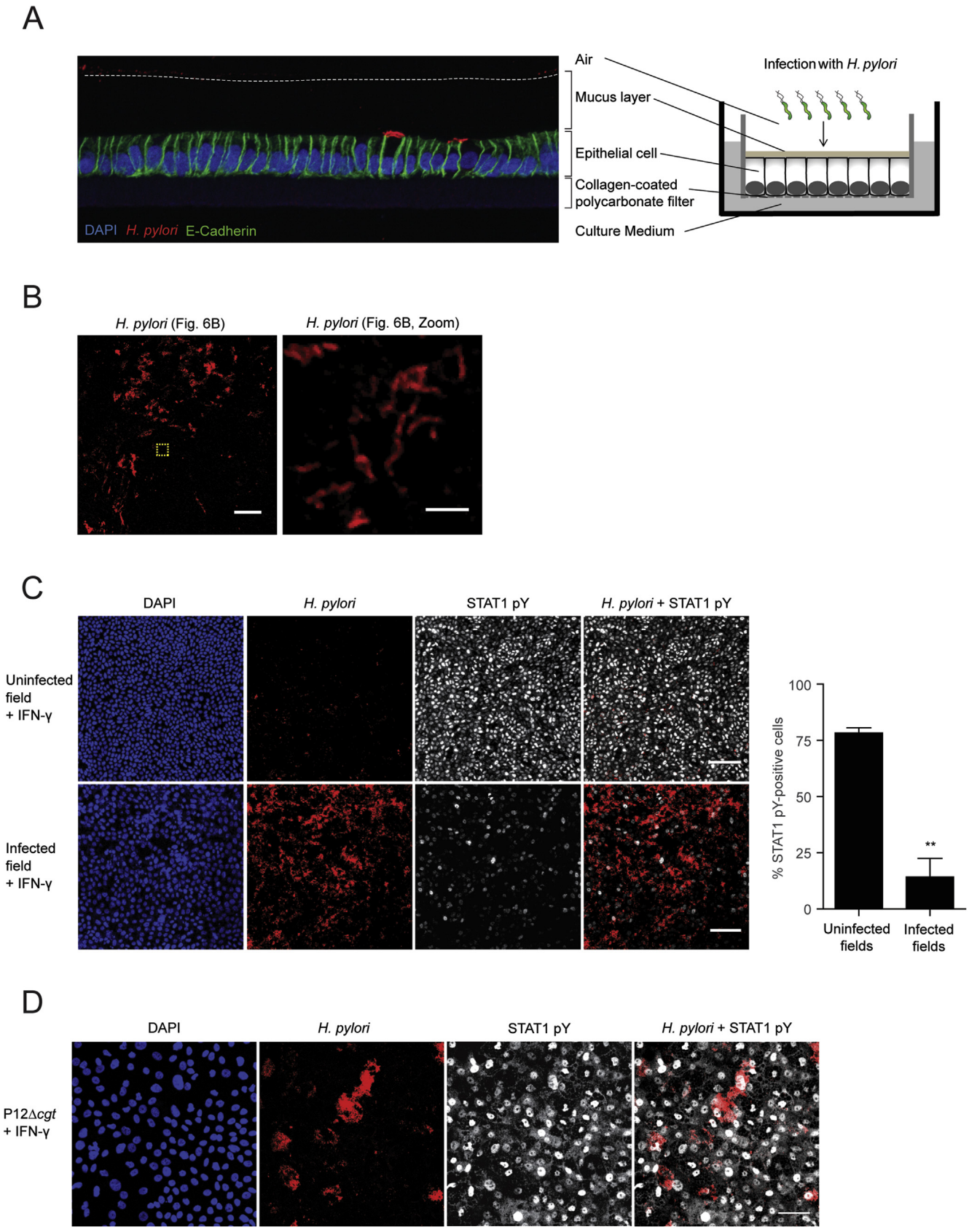
A
Air
Mucus layer
Epithelial cell
Collagen-coated polycarbonate filter
Culture Medium
Infection with H. pylori
DAPI H. pylori E-Cadherin
B
H. pylori (Fig. 6B)
H. pylori (Fig. 6B, Zoom)
C
DAPI
H. pylori
STAT1 pY
H. pylori + STAT1 pY
Uninfected field + IFN-γ
Infected field + IFN-γ
% STAT1 pY-positive cells
100
75
50
25
0
**
Uninfected fields
Infected fields
D
DAPI
H. pylori
STAT1 pY
H. pylori + STAT1 pY
P12Δcgt + IFN-γ

Supplementary Table 1. Primers used in this Study

Primer name	Sequence (5′-3′)
GAPDH Fwd	GGTATCGTGGAAGGACTCATGAC
GAPDH Rev	ATGCCAGTGAGCTTCCCGTTCAG
IRF1 Fwd	ATGCCCATCACTCGGATGC
IRF1 Rev	CCCTGCTTTGTATCGGCCTG
CXCL9 Fwd	ATTGGAGTGCAAGGAACCCC
CXCL9 Rev	GGGCTTGGGGCAAATTGTTT
CXCL10 Fwd	GTGGCATTCAAGGAGTACCT
CXCL10 Rev	GCATCGATTTTGCTCCCCTC
IRF7 Fwd	GAGCTGTGCTGGCGAGAAG
IRF7 Rev	TTGGTTGGGACTGGATCTGC
HP0421 Fwd	GATCGTCGACATGGTTATTGTTTTAGTCGT
HP0421 Rev	GATCAGATCTTTATGATAAGGTTTTAAAGA
Mouse IRF1 Fwd	ATCTCGGGCATCTTTCGCTT
Mouse IRF1 Rev	TCTGCATCTCTAGCCAGGGT
Mouse GAPDH Fwd	TCACCATCTTCCAGGAGCG
Mouse GAPDH Rev	AAGCAGTTGGTGGTGCAGG

Supplementary Figure 5. Blockage of cytokine response in infected ALI cultures. Human gastric primary cells were grown on polycarbonate filters, infected with *H pylori* and analyzed by confocal IF. (*A*) Schematic representation of an infected ALI monolayer. Microscopic image corresponds to a paraffin section of cells infected with P12 at MOI 100 for 3 days. Monolayers were labelled with DAPI and antibodies against cagA (red) and E-cadherin (green) followed by IF analysis. (*B*) Detail at high magnification showing infecting *H pylori* bacteria (labeled in red) from Figure 6*B*. Right image corresponds to the square-delimited area on the left image. Scale bars: 50 μm (left), 5 μm (right). (*C*) Representative microscopic fields from infected filters used for quantification of STAT1 pY-positive cells and quantification of nuclear STAT1 pY-positive cells in infected fields. After 3 days of infection with *H pylori* wild type (MOI 100), cells were treated for 30 minutes with IFNG (10 ng/mL). Filters were labelled with DAPI (DNA, blue), and antibodies against STAT1 pY (white) and *H pylori* (red), followed by whole mount IF. Scale bar: 100 μm. For quantification, microscopic fields homogeneously infected (number of cells n = 9548) were compared with non- or minimally infected ones (number of cells n = 15,682). Results were obtained from 4 independent infected filters and are expressed as percentage of nuclear STAT1 pY-positive cells determined by ImageJ software. $^{**}P < .01$. (*D*) Analysis of STAT1 phosphorylation. After 3 days of infection with *H pylori* P12Δcgt (MOI 200), cells were treated for 30 minutes with IFNG (10 ng/mL), and labelled with DAPI (DNA, blue), and antibodies against STAT1 pY (white) and *H pylori* (red), followed by whole mount IF. *Scale bar*: 50 μm.